THE ANTENNA LABORATORY

RESEARCH ACTIVITIES in ---

Automatic Control *Antennas* *Echo Area Studies*
Microwave Circuits *Astronautics* *E M Field Theory*
Terrain Investigations *Radomes* *Systems Analysis*
Wave Propagation *Submillimeter Applications*

MICROWAVE RADIOMETRIC TEMPERATURES OF TERRAIN

R. L. Riegler

Contract Number NSR-36-008-027

1903-2 30 June 1966

Prepared for:
National Aeronautics and Space Administration
Office of Grants and Research Contracts
Washington, D. C. 20546

Department of ELECTRICAL ENGINEERING

THE OHIO STATE UNIVERSITY
RESEARCH FOUNDATION
Columbus, Ohio

NOTICES

When Government drawings, specifications, or other data are used for any purpose other than in connection with a definitely related Government procurement operation, the United States Government thereby incurs no responsibility nor any obligation whatsoever, and the fact that the Government may have formulated, furnished, or in any way supplied the said drawings, specifications, or other data, is not to be regarded by implication or otherwise as in any manner licensing the holder or any other person or corporation, or conveying any rights or permission to manufacture, use, or sell any patented invention that may in any way be related thereto.

The Government has the right to reproduce, use, and distribute this report for governmental purposes in accordance with the contract under which the report was produced. To protect the proprietary interests of the contractor and to avoid jeopardy of its obligations to the Government, the report may not be released for non-governmental use such as might constitute general publication without the express prior consent of The Ohio State University Research Foundation.

Qualified requesters may obtain copies of this report from the Defense Documentation Center, Cameron Station, Alexandria, Virginia. Department of Defense contractors must be established for DDC services, or have their "need-to-know" certified by the cognizant military agency of their project or contract.

MICROWAVE RADIOMETRIC TEMPERATURES OF TERRAIN

R. L. Riegler

Contract Number NSR-36-008-027

1903-2

30 June 1966

Prepared for:
National Aeronautics and Space Administration
Office of Grants and Research Contracts
Washington, D. C. 20546

REPORT 1903-2

REPORT

by

THE OHIO STATE UNIVERSITY RESEARCH FOUNDATION
COLUMBUS, OHIO 43212

Sponsor	National Aeronautics and Space Administration Office of Grants and Research Contracts Washington, D. C. 20546
Contract Number	NSR-36-008-027
Investigation of	Radar and Microwave Radiometric Techniques for Geoscience Experiments
Subject of Report	Microwave Radiometric Temperatures of Terrain
Submitted by	R. L. Riegler Antenna Laboratory Department of Electrical Engineering
Date	30 June 1966

The material contained in this report is also used as a thesis submitted to the Department of Electrical Engineering, The Ohio State University as partial fulfillment for the degree Master of Science.

ABSTRACT

The concept of radiometric temperature is discussed; special attention is given to the problem of non-ideal antennas and a computer program is given for estimating surface radiation temperature from observed antenna temperature.

Several surface and sky models are discussed and the equations for calculating their radiometric temperatures are given.

Two working microwave radiometers were developed (10 GHz and 35 GHz) and used to measure the radiation temperatures for several types of terrain. Good agreement was obtained between the measured temperatures and temperatures computed from the theoretical models.

CONTENTS

CHAPTER I
INTRODUCTION

Recently there has been considerable interest in the practical application of radiometer systems at microwave frequencies.[1,2,3] Previously the radiometer was an instrument used primarily by the radio astronomer, but it has now found useful application in many other fields. For example,[4] the Coast Guard will soon be using airborne radiometers for iceberg patrol; because icebergs have a lower reflectivity than the surrounding sea they appear hotter to the radiometer. There has also been much work done with radiometers in the area of guidance systems, both for missiles and sea vessels. A practical radiometer sextant has already been developed which is accurate to 10 seconds of arc for solar sights.[4]

Both geologists and agronomists are attempting to use the radiometer as a remote sensor. An appreciation of recent studies in these fields may be obtained from the proceedings of the first three symposia on "Remote Sensing of Environment," held at the University of Michigan.[1,2]

But before these schemes can become practical or meaningful it is necessary to study the radiometer problem on a more fundamental level. That is, the relationship between the radiometric

temperature of a body and its physical and electrical properties must be understood in order to be able to predict the effects of such factors as surface roughness, density, water content, dielectric constant and chemical composition. This requires being able to accurately measure the radiometric temperature of the surface, and thus prohibits the use of many simplifying approximations in the analysis of the data. In particular the assumption of an ideal antenna in the reduction of data introduces significant errors even for antennas which have very good patterns. Extensive work has been done on this antenna problem and a solution has been obtained which corrects for the non-ideal characteristics of the actual antenna used to perform the measurements. In order to verify the theoretical calculations of expected radiometric temperatures and also to study the properties of several terrain types, two microwave radiometers (10 GHz and 35 GHz) were designed and constructed. Several types of terrain, including a series of lavas and a number of crops, were measured and the experimental values of apparent temperature were compared to those predicted from theoretical models.

CHAPTER II
THEORETICAL CONCEPTS OF RADIATION AND THE EFFECT OF A NON-IDEAL ANTENNA

All objects above zero degrees Kelvin emit electromagnetic radiation. The amount of radiation emitted can be calculated quite accurately by using the Rayleigh-Jeans low frequency approximation to Planck's law of radiation. Planck's law for a blackbody radiator is given by the equation

$$J = \frac{2hf^3}{c^2} \Delta f \left[\frac{1}{\epsilon^{\frac{hf}{kT}} - 1} \right] \frac{\text{watts}}{\text{m}^2 - \text{sterad}}$$

where

J = emitted power per unit area of its surface per unit solid angle

c = velocity of light = 3×10^8 meters/sec

h = 6.623×10^{-34} joule-sec (Planck's const)

k = 1.38×10^{-23} joule/°K (Boltzmann's const)

T = thermometric temperature of the radiating body in degrees Kelvin

Δf = incremental bandwidth.

The Rayleigh-Jeans approximation then makes use of the fact that $hf << kT$ for temperatures above a few degrees Kelvin in the

microwave region, to provide a much simpler expression for emitted power. The exponential term can be expanded into a power series; only the first two terms need be retained so that

$$J = \frac{2hf^3}{C^2}\,\Delta f\left[\frac{1}{\frac{hf}{kT}}\right] = \frac{2f^2kT\Delta f}{C^2} = \frac{2kT\Delta f}{\lambda^2} \quad \frac{\text{watts}}{m^2 - \text{sterad}}$$

It is now necessary to relate the power emitted by an object to the power received at the terminals of an antenna. Consider an ideal antenna which has a very small uniform beamwidth Ω_{ant} steradians and no other side or back lobes. The small beam area of the antenna assures that the object will present a constant temperature to the antenna. If the blackbody object is at T_o degrees Kelvin then the power received at the terminals of the antenna is:

$$P_{ant} = \frac{1}{2} J A_{em} \Omega_{ant}$$

A_{em} is the maximum effective collecting aperture of the antenna and is given by

$$A_{em} = \frac{\lambda^2}{4\pi} D_{max} = \frac{\lambda^2}{4\pi} [\text{maximum directivity}].$$

The factor of $\frac{1}{2}$ is due to the assumed randomness of polarization of the emitted radiation, so that only half the incident power will be absorbed by the antenna. Thus

$$P_{ant} = \frac{1}{2}\left[\frac{2kT\,\Delta f}{\lambda^2}\right] A_{em}\,\Omega_{ant} .$$

Using the expression for A_{em} and cancelling

$$P_{ant} = k\,T_o\,\Delta f .$$

Since the standard definition of antenna temperature T_a is given by $P_{ant} = k\,T_a\Delta f$, the antenna temperature at the receiving terminals of the ideal antenna is exactly equal to the physical temperature of the blackbody radiator.

Since blackbody radiators are rarely encountered in practice it is necessary to introduce the concept of equivalent brightness temperature of a real body. The equivalent brightness or apparent radiometric temperature (T_{eq}) of any body is defined as the temperature of an ideal blackbody situated at the same position as the original body and emitting the same radiation intensity to the point of observation. The power density from a real body is then

$$J = \frac{2kT_{eq}}{\lambda^2}\,\Delta f\,\frac{\text{watt}}{\text{m}^2 - \text{sterad}} .$$

Returning again to the relationship between the antenna temperature and the effective brightness temperature, consider an ideal antenna (refer to Fig. 1) which has only a single pencil beam, described by its normalized antenna pattern function $f(\theta', \phi')$.

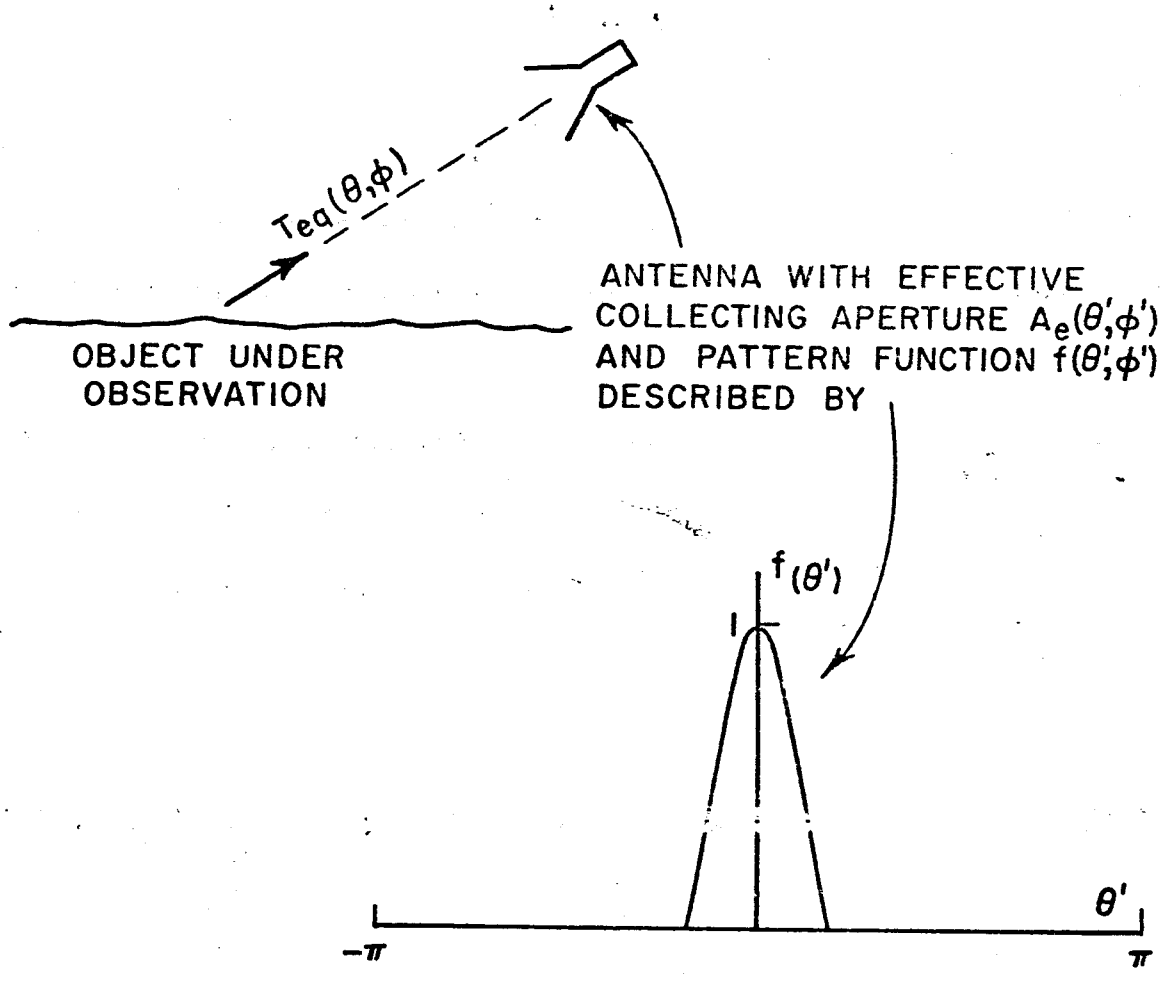

Fig. 1. Ideal antenna assumption.

Assuming that the object under observation is large enough so that its equivalent temperature is constant over the area covered by the antenna beam, the power received at the terminals of the antenna is

$$P_{ant} = \frac{J(\theta,\phi)}{2}\iint A_e(\theta',\phi')d\Omega = 2kT_{eq}(\theta,\phi)\,\frac{\Delta f A_{em}}{2\lambda^2}\iint f(\theta',\phi')d\Omega$$

but

$$A_{em} = \frac{D_{max}\lambda^2}{4\pi} = \frac{\lambda^2}{\iint f(\theta', \phi')d\Omega}$$

so that one obtains $P_{ant} = k\,T_{eq}(\theta, \phi)\,\Delta f$ and the equivalent brightness temperature of the body is equal to the antenna temperature of an ideal antenna.

It must be realized, however, that in practice antennas do not have the ideal pattern assumed above, but in fact accept some radiation from every direction. For this case the equivalent brightness temperature is related to the antenna temperature by*

---

*In fact, Eq. (1) should be replaced by

$$T_{ant}(\theta_o) = \frac{\sum_{i=1}^{2} \int_0^{2\pi} \int_0^{\pi} T_i(\theta) f_i(\theta', \phi') \sin\theta' \, d\theta' \, d\phi'}{\sum_{i=1}^{2} \int_0^{2\pi} \int_0^{\pi} f_i(\theta', \phi') \sin\theta' \, d\theta' \, d\phi'}$$

where $f_1(\theta', \phi')$ is the antenna pattern measured with the design polarization and $T_1(\theta)$ is the temperature of radiation impinging on the antenna with that polarization; $f_2(\theta', \phi')$ is the antenna pattern for polarization state orthogonal to the design polarization and $T_2(\theta)$ is the incident radiation of corresponding polarization. In practice the cross polarized term is small for a well designed antenna, and contributes only a degree or two to T_{ant}.

$$(1) \quad T_{ant}(\theta_o) = \frac{\int_0^{2\pi}\int_0^{\pi} T(\theta)\, f(\theta', \phi') \sin\theta'\, d\theta'\, d\phi'}{\int_0^{2\pi}\int_0^{\pi} f(\theta', \phi')\, \sin\theta'\, d\theta'\, d\phi'}$$

or more generally the antenna temperature is the weighted average of all radiometric temperatures where

$T_{ant}(\theta_o)$ is the antenna temperature in the direction θ_o

$T(\theta)$ is the radiometric temperature distribution

$f(\theta', \phi')$ is the normalized antenna power pattern function which acts as the weighting function

$\sin\theta'\, d\theta'\, d\phi'$ is the element of solid angle.

(Refer to Figs. 5 and 6 for geometry.)

Now the problem to be analyzed is; given the experimentally measured values of antenna temperatures measured with a radiometer system, find the corresponding values of radiometric or brightness temperature.

The best way to solve the problem is to construct an antenna which has a very narrow uniform pencil beam with no sidelobes, backlobes or spillover losses. In this case the antenna temperature is equal to the radiometric temperature. Unfortunately, even antennas which are designed to maximize the energy in the main beam fail to satisfy the ideal antenna assumption.

For example, Fig. 2 shows the pattern of an X-band parabolic reflector antenna specially designed for radiometric applications. Although its pattern appears very close to that of an ideal antenna, a study of Fig. 3, which gives the details of the side and back lobe structure, shows that a significant amount of the received power can be absorbed off the main beam. In order to estimate the actual energy distribution as a function of the polar angle θ, several cuts (E plane, H plane, etc.) were taken to obtain an average $f(\theta)$, and these were then integrated to get the fraction of total power contained in a cone of half angle θ (see Fig. 4).

This real antenna has only about 75% energy in its main beam and it is not until 110 degrees off axis that 99% of the energy has been collected. Clearly the assumption of an ideal antenna (all power in narrow beam) is not valid and it is necessary to find some other way to relate antenna and radiometric temperatures; that is, the effect of radiation entering the antenna through the sidelobes must be considered.

The problem of determining T_{ant}, given $T(\theta)$ is straightforward. In practice however T_{ant} is the measured quantity and $T(\theta)$ is the unknown. To find $T(\theta)$ then it is necessary to solve Eq. (1) as an integral equation. An exact solution cannot be

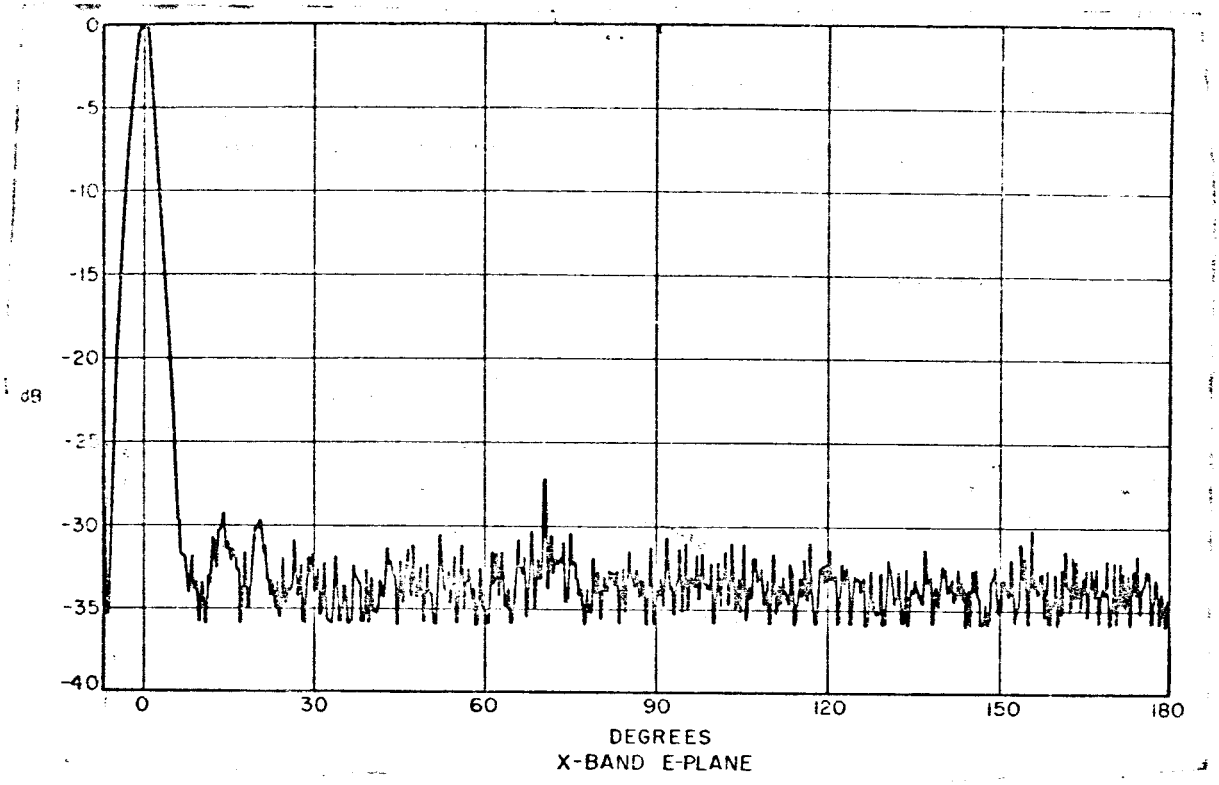

Fig. 2. Typical high gain antenna pattern.

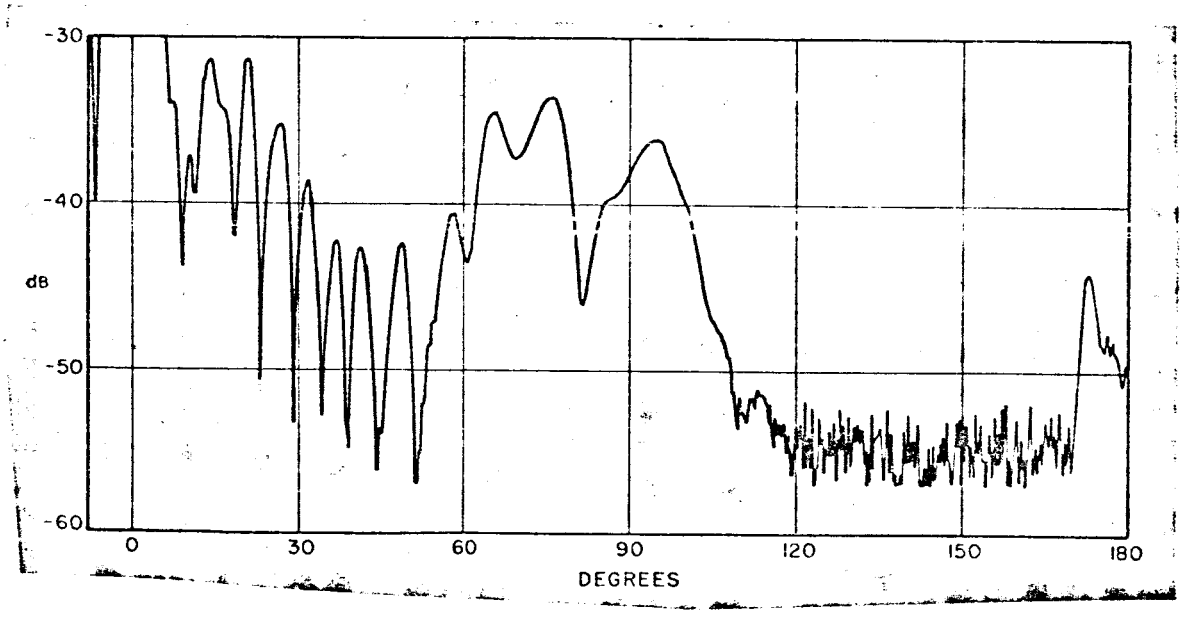

Fig. 3. Antenna sidelobe detail.

obtained unless the antenna temperature is measured for every value of θ, ϕ; in practice a good approximate solution which uses a finite number of measured antenna temperatures is desired.

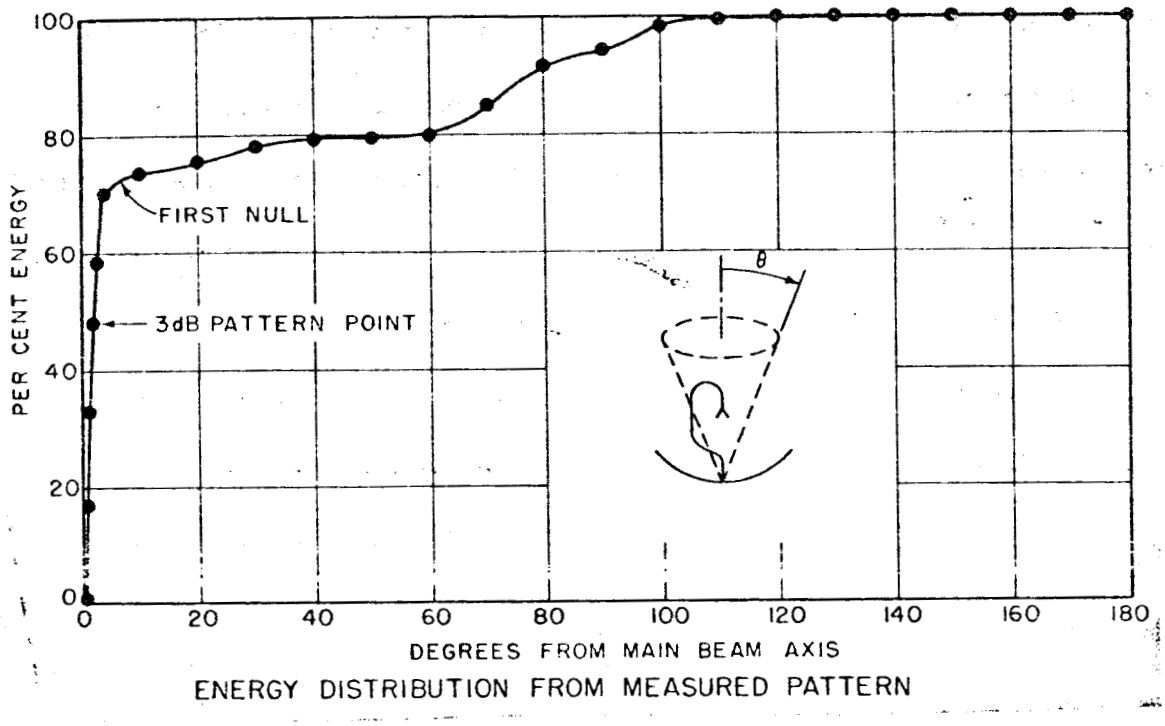

Fig. 4.

The most straightforward solution would be to expand $T(\theta)$ in some type of series, such as a power or Fourier series. Then if T_{ant} were measured, say, every 10°, for $0 \leq \theta \leq 180$ it would be necessary to solve a system of 19 equations with 19 unknowns. Since the coefficients are double integrals the computations are lengthy even for a high speed digital computer, and makes this

type of solution undesirable from an economic viewpoint. However there is another type of approximation which works quite well for antennas with a fairly large fraction of energy in the main beam. The procedure is to use the measured values of antenna temperature to estimate $T(\theta)$. This initial estimate is then put into the integral to see if the equation is satisfied for each value of θ. If it is not, the initial estimate is modified by comparing this computed $T(\theta)$ distribution to the measured T_{ant} distribution, and adjusting the estimate of $T(\theta)$ by the difference between the two values. This iteration technique is repeated until the equation is satisfied, for all $T_{ant}(\theta)$, indicating that a good estimate for $T(\theta)$ has been found. This bootstrap method works quite well; after only two iterations $T(\theta)$ is within a degree or two of its self consistent value. A computer program for the ϕ independent case is given in Appendix III.

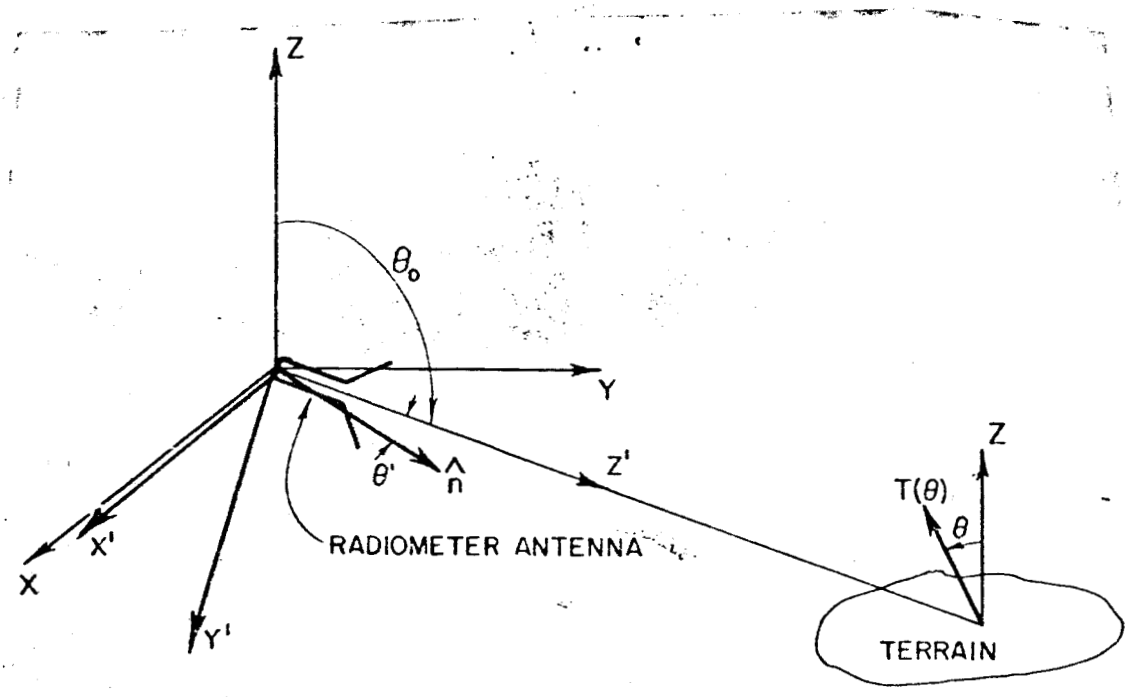

Fig. 5. Geometry of radiometer problem.

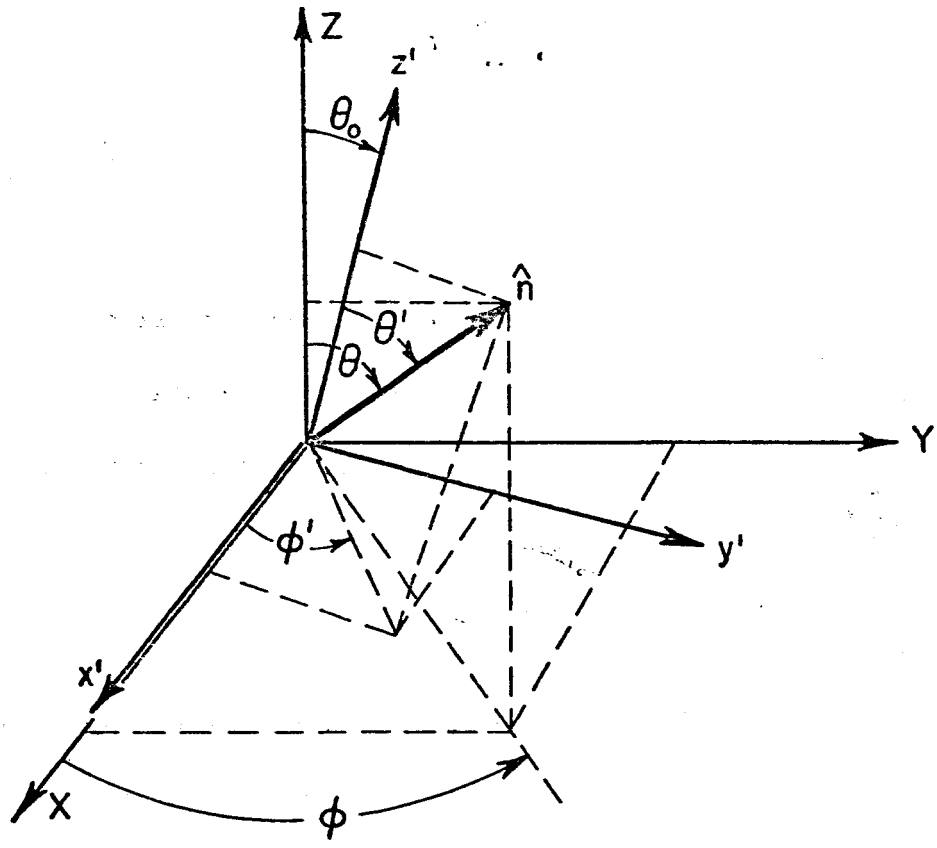

Fig. 6. Coordinate transformation.

CHAPTER III
MODELS

There are several sky and surface models whose radiometric temperature can be predicted. Four of these, which will be discussed in this section, are: the atmosphere, the flat surface, and two rough surfaces.

Sky Model

In the microwave region almost all of the atmospheric radiation is due to oxygen and water vapor absorption. The percentage of oxygen in the atmosphere remains almost constant as a function of time but the water vapor content may have a seasonal variation of twenty to one;[5] hence the radiometric temperature of the sky is not a constant, but if the pressure, temperature, and water vapor are known the attenuation per unit length and hence the radiometric temperature can be computed using formulas derived by Van Vleck.[6]

The most commonly used model for determining sky temperature distributions is to assume a planar earth; for this case the path length over which absorption occurs is proportional to the secant of the angle from zenith. This assumption of a plane earth gives good accuracy for angles less than about 80° from zenith.

A convenient form for determining the sky temperature as a function of angle is given by Wulfsberg[5]

$$T_{sky}(\theta) = (1 - \alpha_o^{\text{secant }\theta}) T_m \qquad (2)$$

where

α_o is fractional transmission of atmosphere at zenith ($\theta = 0$)

T_m is the mean absorption temperature, which for clear sky conditions can be expressed as $T_m = 1.12\ T_{ground} - 50°K$.

Extensive experimental measurements of sky temperature at several microwave frequencies have been made by Air Force Cambridge Laboratories[5] under various meteorological conditions and the results agree quite well with calculations based on this simple model.

Smooth Surfaces

Another model which can be analyzed quite easily is the very smooth surface. Consider an antenna looking at a smooth planar surface at some angle of incidence θ. For terrestrial surfaces the transmissibility is zero so that the radiometric temperature is composed of two components, radiation which is emitted by the surface, and radiation from the atmosphere which is reflected by the surface.

The radiometric temperature can then be computed from the reflection coefficient since[8]

$$T_{rv} = |\dot{r}_v|^2 \, T^v_{sky}(\theta) + (1 - |\dot{r}_v|^2) \, T_g$$

$$T_{rh} = |\dot{r}_h|^2 \, T^h_{sky}(\theta) + (1 - |\dot{r}_h|^2) \, T_g$$

where

$\dot{r}_v, \dot{r}_h$ = reflection coefficient for vertical and horizontal polarization

T_{rv}, T_{rh} = vertically and horizontally polarized components of radiometric temperature

$T^v_{sky}(\theta_o), T^h_{sky}(\theta_o)$ = vertically and horizontally polarized components of radiometric sky temperature in direction θ_o

T_g = thermodynamic temperature of object.

The reflection coefficients are[7]

$$\dot{r}_h = \frac{\dot{\mu} \cos\theta_o - \mu_o \sqrt{\omega^2 \dot{\mu}\dot{\epsilon} - k_o^2 \sin^2\theta_o}}{\dot{\mu} \cos\theta_o + \mu_o \sqrt{\omega^2 \dot{\mu}\dot{\epsilon} - k_o \sin^2\theta_o}}$$

$$\dot{r}_v = \frac{\dot{\epsilon} \, k_o \cos\theta_o - \epsilon_o \sqrt{\omega^2 \dot{\mu}\dot{\epsilon} - k_o^2 \sin^2\theta}}{\dot{\epsilon} \, k_o \cos\theta_o + \epsilon_o \sqrt{\omega^2 \dot{\mu}\dot{\epsilon} - k_o^2 \sin^2\theta}}$$

where

$\dot{r}_h$ = complex reflection coefficient for horizontal polarization

$\dot{r}_v$ = complex reflection coefficient for vertical polarization

$\dot{\mu}$ = complex permeability of object

$\dot{\epsilon}$ = complex dielectric constant of object

μ_o = free space permeability

ϵ_o = free space permittivity

$k_o^2 = \omega^2 \mu_o \epsilon_o$.

A case of particular interest is when the object is non-magnetic, that is $\dot{\mu} = \mu_o$. Under this condition the radiometer equations for a smooth surface reduce to

$$T_{rh} = \left| \frac{\cos\theta_o - \sqrt{\epsilon_r - \sin^2\theta_o}}{\cos\theta_o - \sqrt{\epsilon_r - \sin^2\theta_o}} \right|^2 T^h_{sky}(\theta_o) + \left[1 - \left| \frac{\cos\theta_o - \sqrt{\epsilon_r - \sin^2\theta_o}}{\cos\theta_o + \sqrt{\epsilon_r - \sin^2\theta_o}} \right|^2 \right] T_g$$

(3)

$$T_{rv} = \left| \frac{\epsilon_r \cos\theta_o - \sqrt{\epsilon_r - \sin^2\theta_o}}{\epsilon_r \cos\theta_o + \sqrt{\epsilon_r - \sin^2\theta_o}} \right|^2 T^v_{sky}(\theta_o) + \left[1 - \left| \frac{\epsilon_r \cos\theta_o - \sqrt{\epsilon_r - \sin^2\theta_o}}{\epsilon_r \cos\theta_o + \sqrt{\epsilon_r - \sin^2\theta_o}} \right|^2 \right] T_g$$

where $\epsilon_r = \frac{\dot{\epsilon}}{\epsilon_o}$ relative dielectric constant.

It is interesting to note that the reflection coefficient for vertical polarization is zero when $\tan\theta = \sqrt{\epsilon_r}$ (Brewster's angle) and for this particular angle the radiometric temperature should be exactly equal to the thermal temperature of the object.

Rough Surfaces

The apparent temperature of two simple types of rough (diffusely scattering) surfaces can also be predicted if the bistatic scattering characteristics of the surface are known. For a surface whose bistatic scattering cross-section per unit area can be approximated by

$$\sigma_o(\theta_o, \theta_s) = \frac{\gamma_o}{2}[\cos\theta_o + \cos\theta_s]$$

(i.e., for which the backscattering or radar cross section is $\sigma_o(\theta) = \gamma_o \cos\theta$), the emissivity is[8]

$$\epsilon = 1 - \frac{\gamma_o}{4}\left(1 + \frac{\text{secant } \theta}{2}\right)$$

where γ_o is a constant determined from the radar backscattering measurements of the surface.

Thus the apparent temperature of the rough surface using this scattering model is

$$(4) \quad T_r^{h,v} = \left[1 - \frac{\gamma_o^{h,v}}{4}\left(1 + \frac{\text{secant } \theta_o}{2}\right)\right] T_g + \left[\frac{\gamma_o^{h,v}}{4}\left(F_1(\alpha_o) + \frac{F_2(\alpha_o)\ \text{secant } \theta_o}{2}\right)\right] T_m$$

where the superscripts represent the horizontal and vertical component respectively and

$$F_1(\alpha_o) = 1 - \alpha_o + \ell n\, \alpha_o\, E_i\, (\ell n\, \alpha_o)$$

$$F_2(\alpha_o) = 1 - \alpha_o - \alpha_o \ell n\, \alpha_o + (\ell n\, \alpha_o)^2\, E_i(\ell n\, \alpha_o)$$

$E_i(\ell n\, \alpha_o)$ = exponential function, tabulated in Reference 12.

Similarly for a Lambert Law surface, for which $\sigma_o(\theta_o, \theta_s) = \gamma_L \cos\theta_o \cos\theta_s$ and backscattering cross-section per unit area $\sigma_o(\theta) = \gamma_L \cos^2\theta$, the emissivity is given by

$$\epsilon = 1 - \frac{\gamma_L}{4}$$

and the apparent temperature is

$$(5) \qquad T_r^{h,v} = \left(1 - \frac{\gamma_L^{h,v}}{4}\right) T_g + \frac{\gamma_o^{h,v}}{4} F_2(\alpha_o)\ T_m \ .$$

Appendix I contains measured surface temperatures and the corresponding theoretical temperatures for all of the models discussed in this chapter.

CHAPTER IV
RADIOMETER DESIGN

A. System Description

The design of a radiometer is determined largely by its intended use. For example a radiometer intended for radio astronomy must be able to detect temperature differences in the order of 0.01°K while a radiometer used for terrain mapping measurements requires a sensitivity of only a degree or two. The X-band and K_a-band radiometers discussed in this report were designed specifically for terrain measurements so that the comments and design procedures apply to this particular type of radiometer.

The purpose of any radiometer is to accurately measure the amount of power radiated by an object. The thermal power in the microwave region which is radiated by the object must be received by some type of antenna and processed to obtain an output which is related to the radiometric temperature of the body under observation. A system which performs this function quite well is shown below in Fig. 7. The system is called a commutating comparison or Dickey radiometer.

The commutating component is a microwave ferrite switch which alternately switches the input of the receiver between an

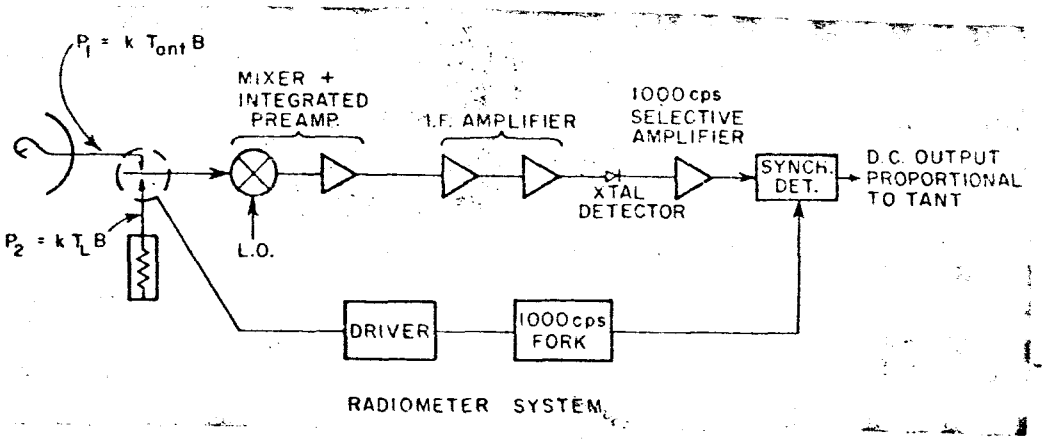

Fig. 7. Radiometer system.

antenna, which presents a noise power $k\,T_{ant}B$, and a matched microwave termination at temperature T_L, which delivers a noise power $k\,T_L B$. This modulation process continuously compares the known temperature of the reference load to the unknown antenna temperature. A balanced microwave mixer is used to down-convert the noise signal to an IF frequency where it is amplified.

At the crystal detector, the envelope of the signal, which contains the desired information is recovered, amplified, and synchronously detected to provide a dc voltage output proportional to the antenna temperature.

B. System Sensitivity

The usual criterion to evaluate the performance of a radiometer is its minimum detectable temperature sensitivity ΔT. This is the root mean squared value of the fluctuation of the measured values of radiometric temperature.

The expression for ΔT is given by:[9]

$$\Delta T = \kappa \frac{(F-1)\,T_L}{\sqrt{B\tau}} + \frac{G(t)-G_o}{G_o} (T'_L - T_{ant})$$

where

κ = constant depending on modulation, background radiation, detection factors, and other system parameters.

T_L = reference load temperature

T'_L = load temperature referred to mixer input

T_{ant} = effective antenna temperature

F = system noise figure

B = predetection bandwidth

τ = postdetection integration time

$G(t)$ = instantaneous gain

G_o = average value of gain.

Thus the system sensitivity is composed of two parts, a component due to statistical fluctuations and a component due to gain variations. The portion due to gain variation is exceedingly difficult

to measure because it requires accurately knowing the system gain as a function of time. However, for terrain measurements the antenna temperature is close enough to the reference temperature so that the statistical variation term becomes dominant. This assumption has been varified experimentally; the measured value of ΔT is very close to the expected value from the statistical portion alone.

C. Noise Figure

The system noise figure was obtained by the following technique.

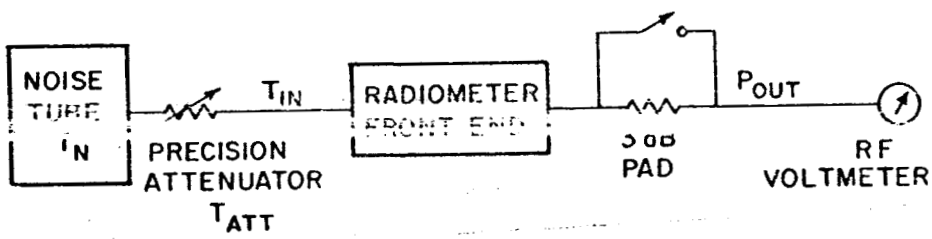

Fig. 8. System for measuring noise figure.

Using the system of Fig. 8, with the noise generator turned off, the precision attenuator set to maximum attenuation, and the 3 db pad shorted, the power delivered to the voltmeter will be

$$P_1 = k T_{att} B G + (F-1) k T_o B G$$

F = noise figure of system

T_{att} = attenuator temperature

T_o = AIEE standard 290°K

B = system bandwidth

G = system gain.

The noise tube is then turned on and the short circuit is removed from the 3 db pad. The precision attenuator is adjusted so that the RF voltmeter reads the same as before. For this condition the output power P_2 from the amplifier which is delivered to the 3 db pad is

$$P_2 = k T_{IN} BG + (F-1) k T_o BG$$

where

$$T_{IN} = \alpha T_N + (1-\alpha) T_{att}$$

α = attenuator factor ($\alpha < 1$).

But $P_2 = 2P_1$ since the 3 db pad has been added so that one obtains

$$F = 1 + \frac{T_{IN} - 2 T_{att}}{T_o}$$

This method of measuring noise figure has the advantage that the noise bandwidth and gain of the system need not be determined; also, the linearity and calibration of the RF voltmeter is of no concern.

D. Summary of Performance

The performance of the two radiometer systems constructed can best be understood by examining a summary of their characteristics.

Summary of Radiometer Characteristics

	X-Band	K_a-Band
1. Calculated ΔT sensitivity with 5 seconds integration time and radiometer constant k = 5	.48°K	.96°K
2. Measured ΔT sensitivity with same integration time	.75°K	1.5°K
3. Measured noise bandwidth (double sideband)	350 MHz	350 MHz
4. Measured noise figure	12.5 ± 0.5 db	15.7 ± 0.5 db
5. Antenna beamwidth	(3.5)	(1.5)
6. Antenna VSWR (maximum over frequency range used)	1.09	1.10
7. Oven load VSWR (see Fig. 12)	1.05	1.06
8. Reference load VSWR	1.02	1.05
9. Predetection power gain	60 db	60 db
10. Postdetection voltage amplification	10^5	10^5

CHAPTER V
CALIBRATION

A. System Parameters

The usual calibration method is to refer all temperatures to the input of the mixer; this requires accurately measuring the losses of all waveguide from antenna to the mixer, and the attenuation characteristics of the ferrite switch.

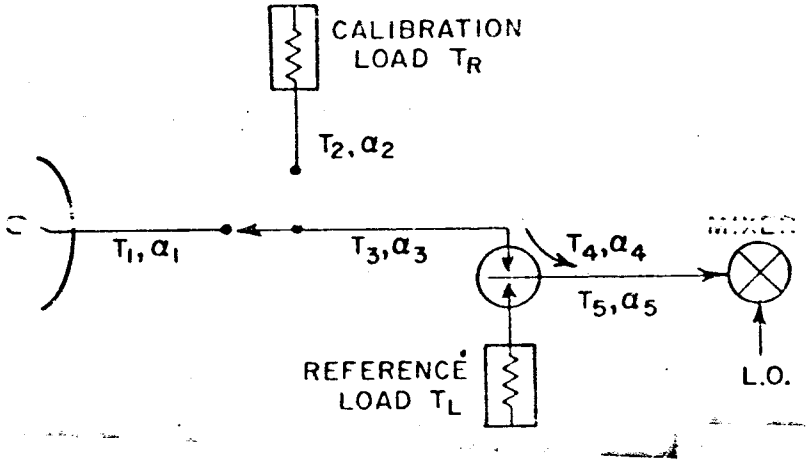

Fig. 9. Calibration of radiometer.

Referring to Fig. 9 the equivalent temperature at the mixer input with the antenna connected is

$$T_{mix_1} = \alpha_5[\alpha_4[\alpha_3[\alpha_1 T_{ant} + (1-\alpha_1) T_1] + (1-\alpha_3) T_3] + (1-\alpha_4) T_4]$$
$$+ (1-\alpha_5) T_5 + \text{leakage terms from ferrite switch}$$

where

$T_{1,2,3,4,5}$ are the thermal temperatures of the waveguide

$\alpha_{1,2,3,5}$ = attenuation factors of guide

α_4 = attenuation factor of ferrite switch.

A similarly complicated expression is necessary to calculate T_{mix_2}, the temperature at the input of the mixer when the calibration load is connected. It should be noted that both of these expressions are linear as long as the waveguide temperature and ferrite switch characteristics do not change during the measurement.

i.e., $T_{mix_1} = C_1 T_{ant} + C_2$

$T_{mix_2} = C_3 T_R + C_4$.

The fact that the system is linear can be utilized to reduce the number of tedious measurements necessary and eliminate the associated experimental errors. The linearity of the actual system can easily be determined by using a calibrated precision attenuator as shown in Fig. 10.

For this arrangement

$T = \alpha T_{ant} + (1-\alpha) T_o = K_1 V_{out} + K_2$ if system is linear

rearranging $T = \alpha (T_{ant} - T_o) + T_o = K_1 V_{out} + K_2$. Solving for V_{out}

$$V_{out} = \alpha \underbrace{\left[\frac{(T_{ant} - T_o) + T_o - K_2}{K_1}\right]}_{\text{constants during measurement}}$$

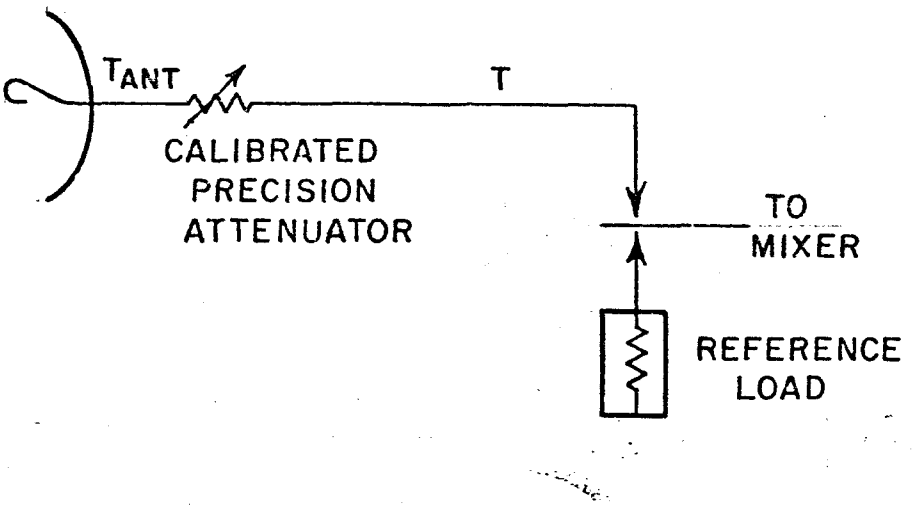

Fig. 10. Determining linearity.

Hence by pointing the antenna at the zenith sky (by far the most convenient low temperature reference) and measuring the radiometer output voltage as a function of attenuator setting, it is possible to check the linearity over the complete dynamic range for which the system is to be used. Such a graph is shown in Fig. 11. The rms deviation from a straight line is of the order of ΔT. Note that the actual value of sky temperature, T_{ant}, or system parameters need not be known.

After the linearity verification it is possible to calibrate the radiometer by referring all temperatures to any common point in the system. The most convenient reference place is at the terminals of the antenna; that is, the radiometer is calibrated to measure

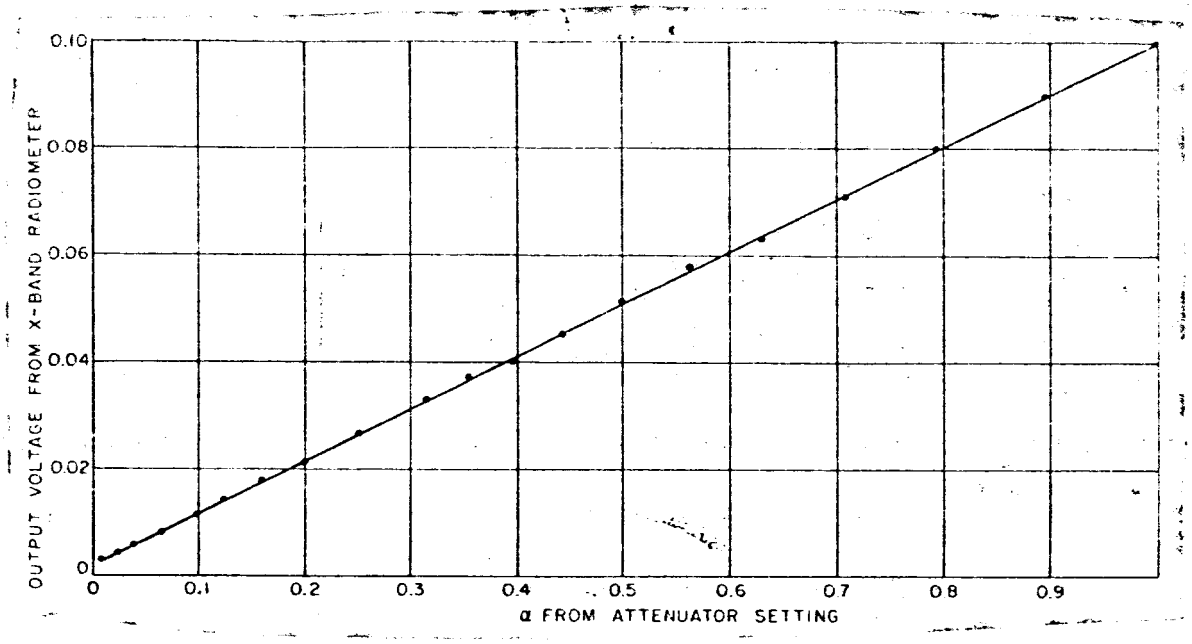

Fig. 11. Verification of linearity.

antenna temperature directly, instead of mixer input temperature. Then from the directly measured values of antenna temperature, the computer program can be used to solve for the desired radiometric temperature.

Referring again to Fig. 9 the calibration equation is

$$T_{calib} = \frac{\alpha_1 T_R + (1-\alpha_1)\, T_1 - (1-\alpha_2)\, T_2}{\alpha_2}$$

where T_{calib} is the value of the calibration temperature T_R referred to the antenna and α_1 is the lumped value of waveguide loss plus insertion loss of calibration switch.

For the practical case of the system remaining at constant temperature during the measurement period, $T_2 = T_1 = T_o$ (the waveguide temperature),

$$T_{calib} = \frac{\alpha_1 T_R + T_o(\alpha_2 - \alpha_1)}{\alpha_2}$$

In this expression the values of α_1, α_2, T_o, and T_R (the temperature of the calibration load) are known and the value of V_{out} corresponding to T_R is measured. Two values of T_R and their corresponding output voltages are necessary and sufficient for calibration.

B. Calibration Techniques

The calibration procedure should be kept simple yet accurate. At X-band the zenith sky temperature is known quite well for a clear sky and can be used to provide a calibration point. At K_a band however the zenith sky temperature depends too much on such factors as relative humidity and cloud cover to provide a suitable reference temperature. It then becomes necessary to obtain other calibration sources.

One method is to construct a microwave blackbody radiator and maintain its temperature at a fixed value. A device which comes very close to this ideal radiator is shown in Fig. 12.[11]

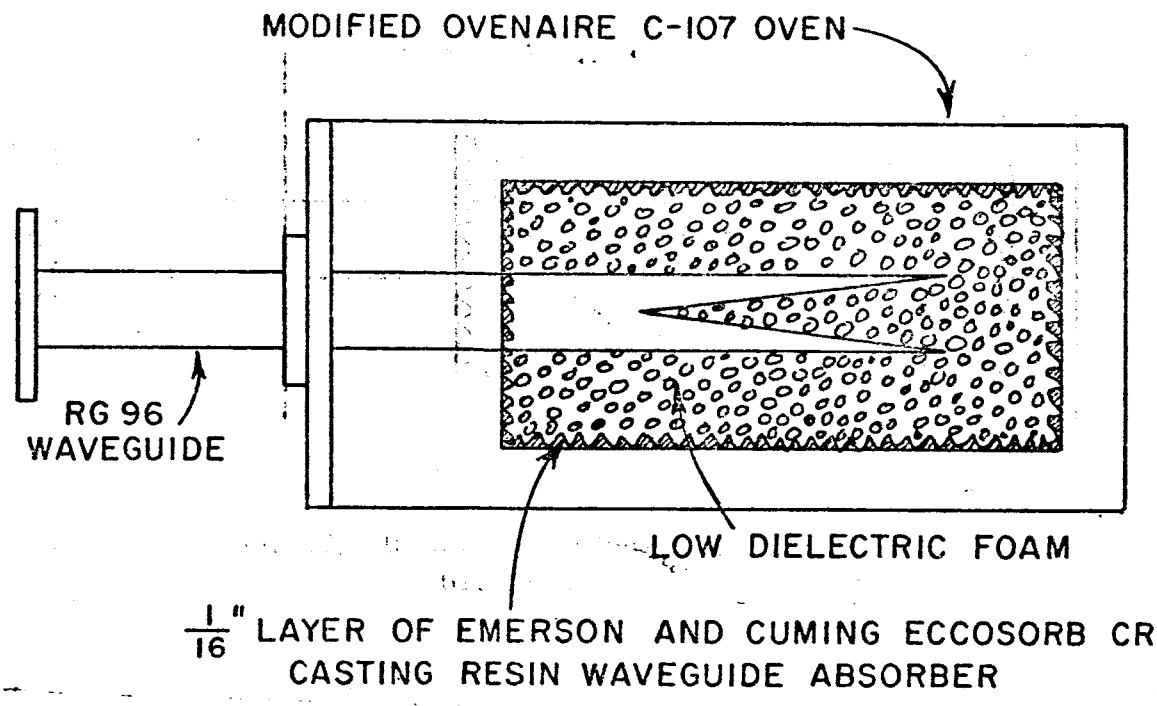

Fig. 12. Calibration source.

It consists of a cylindrical cavity whose surface is coated with a microwave absorber and maintained at a constant temperature of 85°C by the oven. The RG-96 waveguide inside the cavity acts as an antenna to receive the radiation and is tapered to reduce any mismatch due to sharp discontinuities.

The radiation mechanism within the cavity can be understood by considering what happens to energy entering the cavity from the antenna. Any such energy is partly absorbed and partly scattered at the cavity surface. The scattered radiation (see Fig. 13) is repeatedly reflected off the cavity walls. Each time it strikes the

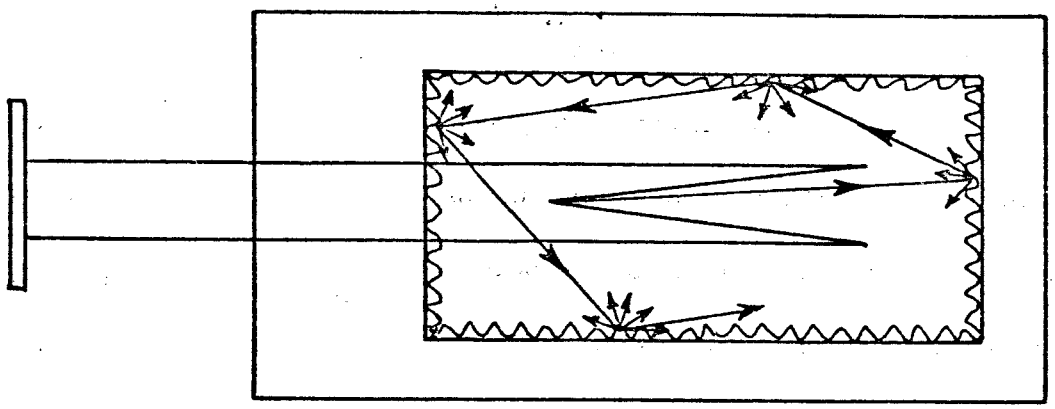

Fig. 13. Radiation mechanism inside calibration source.

wall, part of it is absorbed so that only a negligible fraction ever returns to the antenna. Thus the cavity acts like a black body; practically all of the incident radiation is absorbed. From Table I the input VSWR is 1.05 indicating that less than one tenth of one percent of the incident energy is reflected.

By Kirchoff's Law, the cavity has an emissivity equal to its absorption coefficient (i.e., $\epsilon = 0.999$) so that the "antenna" temperature of the waveguide is very nearly the oven temperature.

This device can be used to provide a known reference at two temperatures, ambient with the oven off, and 358°K with the oven on and in thermal equilibrium. The waveguide can be thermally isolated to prevent any heat transfer between the oven and the waveguide (but not affect the microwave radiation mechanism) by

filling the cavity with a low loss foam. This method seems to be superior to the conventional technique of placing a commercial waveguide termination inside an oven; large temperature gradients usually exist between the waveguide and the oven walls so that the temperature of the radiating material inside the waveguide enclosure is hard to determine accurately and there is also the disadvantage of excessive heat flow down the waveguide.

CHAPTER VI
DISCUSSION OF DATA

This section presents a number of measurements of selected terrain and sky, partly as a catalog, and partly to confirm the approach to interpretation of radiometric temperature previously discussed. All data has been corrected for antenna pattern effects according to Eq. (1) and Appendix III.

The first group of measurements are the sky profiles at X-band (Fig. 14) and K_a-band (Fig. 15). Both measured curves show good agreement with calculated curves and with measurements made by others for normal atmospheric conditions.[5] At K_a-band the rms deviation is about 2.5°K, which is compatible with the radiometer ΔT, uncertainties in calibration, and other experimental errors. At X-band the zenith sky was used as a calibration reference, fixing its value at 5°K; however, with this one point fixed the agreement of temperature versus angle is good.

The second group of data is for a smooth surface, where the scattering is specular and the temperature can be computed from Eq. (3). Figure 16 shows the theoretical and measured temperature of asphalt, which has a dielectric constant of $4.3 + j.1$ at X-band and $2.5 + j.65$ at K_a-band. Both the directly measured

values of antenna temperature (labelled "antenna") and the corresponding computer-corrected surface radiation temperature (labelled "experimental"), are presented, in order to emphasize the significant errors which would occur if the antenna pattern corrections were ignored (compare, for example, Reference 10).

For both frequencies (Figs. 16 and 17) the Brewster angle effect is quite noticeable and the angle at which is occurs is in good agreement with that predicted by Eq. (3) in Chapter III.

The third group consists of vegetated surfaces which, on the basis of a number of radar measurements[13] are known to be rough (scatter isotropically). Thus Eq. (4) can be used to predict their apparent temperature if the scattering parameter γ_o is known. For the particular surfaces whose temperatures are given in Figs. 18-20, special radar measurements were made concurrently with the radiometer measurements. From these, values of γ_o were obtained in each case and appear on each figure. It is seen that the agreement between the radiation temperature and that predicted by Eq. (4) is quite good, except perhaps for the oats; this can be explained in terms of the radar measurements — the oats scattered less isotropically than the wheat and alfalfa so that the empirical model for the scattering law was not as well satisfied as it was for the other crops.

The last group consists of four types of volcanic materials which have about the same chemical composition but quite different physical properties. The materials, lapilli, pumice (2 types), and obsidian are all located near the Mono Crater chain in California. The lapilli was measured on a level area at the north end of the chain, the pumice was measured in a mine situated in the middle of the chain, and the obsidian was measured at the Obsidian Dome, south of the chain. Although all of the substances are more than 70% silicates (predominately SiO_2) there are considerable differences in the density and hence dielectric constant, so that there are significant differences in their apparent temperatures. The lapilli (refer to photo, Fig. 27) is composed of small particles, in the order of 0.5 cm to 1 cm, and its radiometric temperature curve is similar to that of a smooth surface at X-band; at K_a-band, however, it is characteristic of neither a smooth nor a rough surface. This is consistent with the fact that the surface scattering should change its character when the wavelength approaches the surface particle size.

As can be seen from Figs. 23, 24, 25 and 26 both types of pumice (light and dark colored) and the obsidian have apparent temperatures which do not change significantly with look angle, the characteristic of a rough surface. This is to be expected in view

of the fact that the blocks of material were as much as 2 or 3 feet in diameter. The radar scattering characteristics of the dark pumice varied in a manner intermediate between the predictions of Eqs. (4) and (5). Thus the predicted apparent temperature was computed for both models. As seen from Figs. 23 and 24 the measured values of apparent temperature, for both X-band and K_a-band, also lie between those calculated from the two models.

It is interesting to note that the apparent temperatures of the materials follow the trend that would be expected on the basis of their densities; that is, as the density is increased, so is the dielectric constant and the reflectivity, so that the emissivity and thus surface temperature decreases.

CHAPTER VII
CONCLUSION

This report has analyzed the integral relationship between the antenna temperature, which is measured by a radiometer, and the desired radiometric temperature of a surface.

A computer program was developed to convert the measured values of antenna temperature to corresponding values of radiometric temperature, and used to demonstrate that this antenna pattern correction is many times larger than the temperature sensitivity of current radiometer systems. Thus radiometric measurements made by different observers of a particular surface cannot be compared unless the complete pattern of each antenna is known and the necessary corrections made.

Two microwave radiometers were constructed and used to show that good agreement could be obtained between computer-corrected measured temperatures and temperatures computed from theoretical models for several different types of terrain.

A series of rhyolitic lavas was measured and it was verified that changes in density were well correlated with changes in radiometric temperature. Hence, if a surface is known to be of this type, the relative density can be determined remotely by radiometric measurements.

REFERENCES

1. Vivian, Weston, "Passive Microwave Technology and Remote Sensing," Proceedings of the First Symposium on Remote Sensing of Environment, 13-15 February 1962, The University of Michigan.

2. Conway, W. H. and Sakamoto, R. T., "Microwave Radiometer Measurements Program," Proceedings of the Third Symposium on Remote Sensing of Environment, 14-16 October 1964, The University of Michigan.

3. Barath, F. T., "Microwave Radiometry and Application to Oceanography," Oceanography from Space, Proceedings of Conference on the Feasibility of Conducting Oceanographic Exploration from Aircraft, Manned Orbital, and Lunar Laboratories, 24-28 August 1964, Woods Hole, Massachusetts.

4. Microwaves Magazine, July 1965, p. 6.

5. Wulfsberg, Karl N., "Apparent Sky Temperatures at Millimeter-wave Frequencies," Physical Sciences Research Papers No. 38, July 1964, Air Force Cambridge Research Laboratories.

6. Van Vleck, J. H., Propagation of Short Radio Waves, MIT Radiation Laboratory Series.

7. Stratton, J. A., Electromagnetic Theory, Chapter IX, McGraw-Hill Book Company.

8. Chen, Sinclair and Peake, W. H., "Apparent Temperatures of Smooth and Rough Terrain," IRE Transactions on Antennas and Propagation, Vol. AP-9, No. 6, November 1961.

9. Drake, F. D. and Ewen, H. I., "A Broadband Microwave Source Comparison Radiometer for Advanced Research in Radio Astronomy," Proceedings of the IRE, January 1958, p. 53.

10. Straiton, A. W., Tolbert, C. W., Britt, C. O., "Apparent Temperature Distributions of Some Terrestrial Materials and the Sun at 4.3 mm Wavelength," Jour. Appl. Phys. 29, 776, 1958.

11. Hornak, D. E. and Wilt, R. E., "Millimeter Wave Radiometer Program," Sperry Microwave Electronics Co.

12. Jahnke and Emde, Tables of Functions, Dover Publications.

13. Cosgriff, R. L., Peake, W. H. and Taylor, R. C., "Terrain Scattering Properties for Sensor System Design," (Terrain Handbook II), May 1960, The Ohio State University Engineering Experiment Station, EESB 181.

ACKNOWLEDGMENTS

The author would like to thank Dr. W. H. Peake for his many contributions, both during the development of the radiometer systems and in the preparation of this report. The valuable suggestions by Dr. C. H. Walter were also appreciated. Many of the radiometric temperatures were made by Mr. Beau A. Hamer and Mr. David K. Landis and their contribution is gratefully acknowledged.

APPENDIX I

DATA

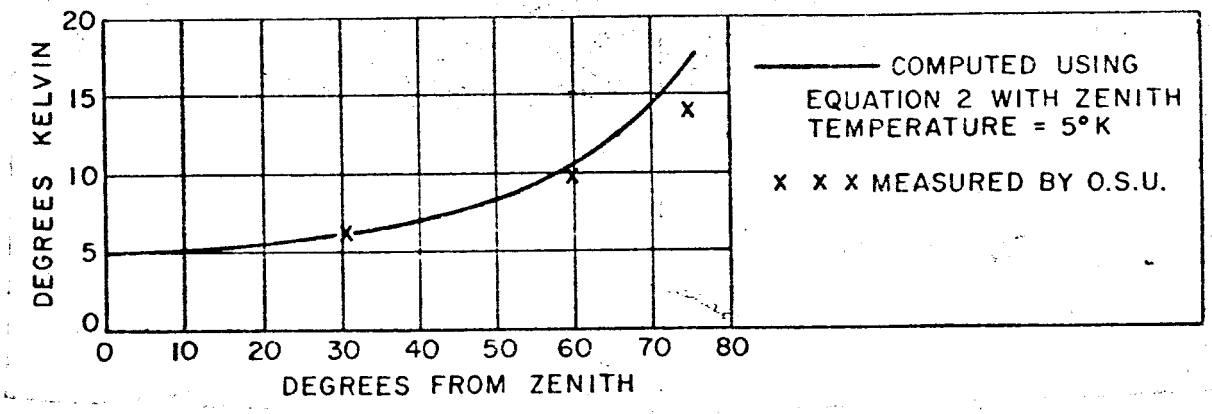

Fig. 14. X band sky profile.

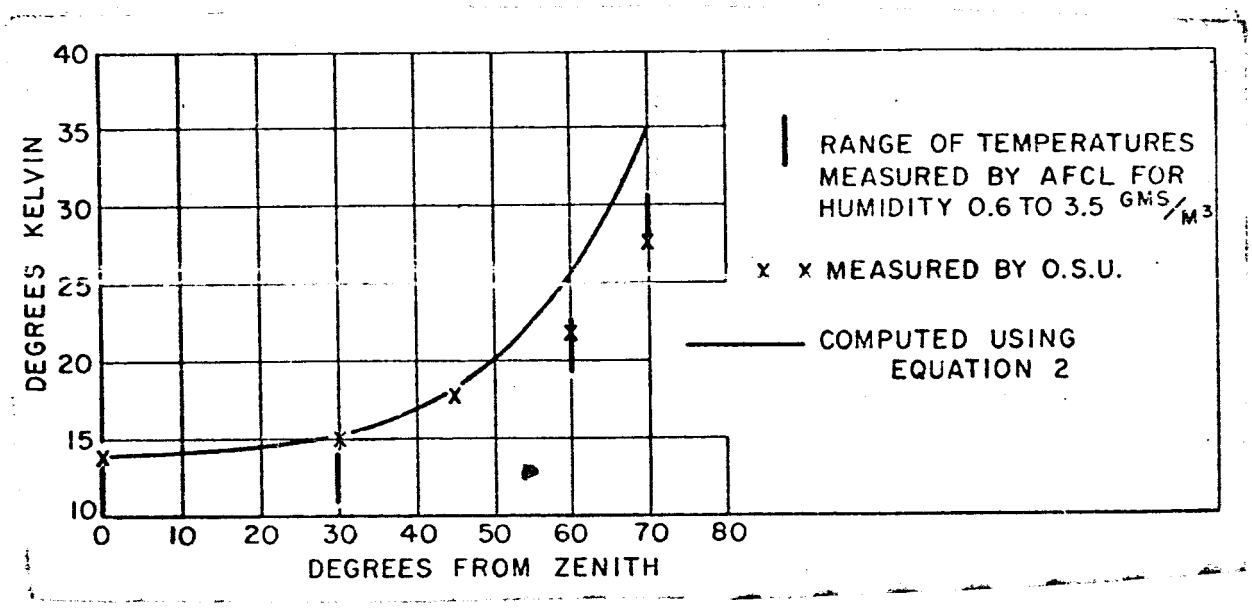

Fig. 15. K_a band sky profile.

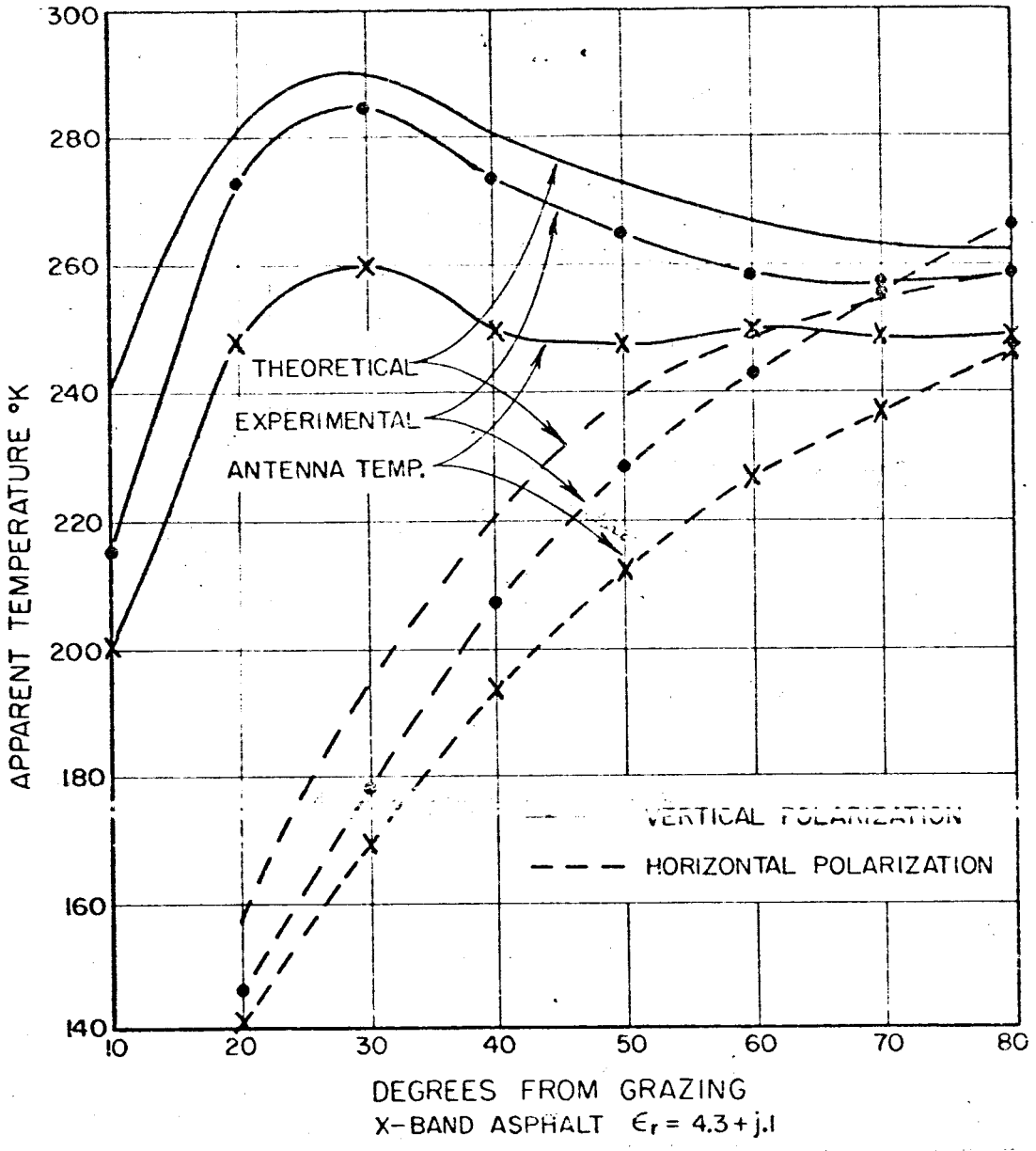

Fig. 16. X-band asphalt.

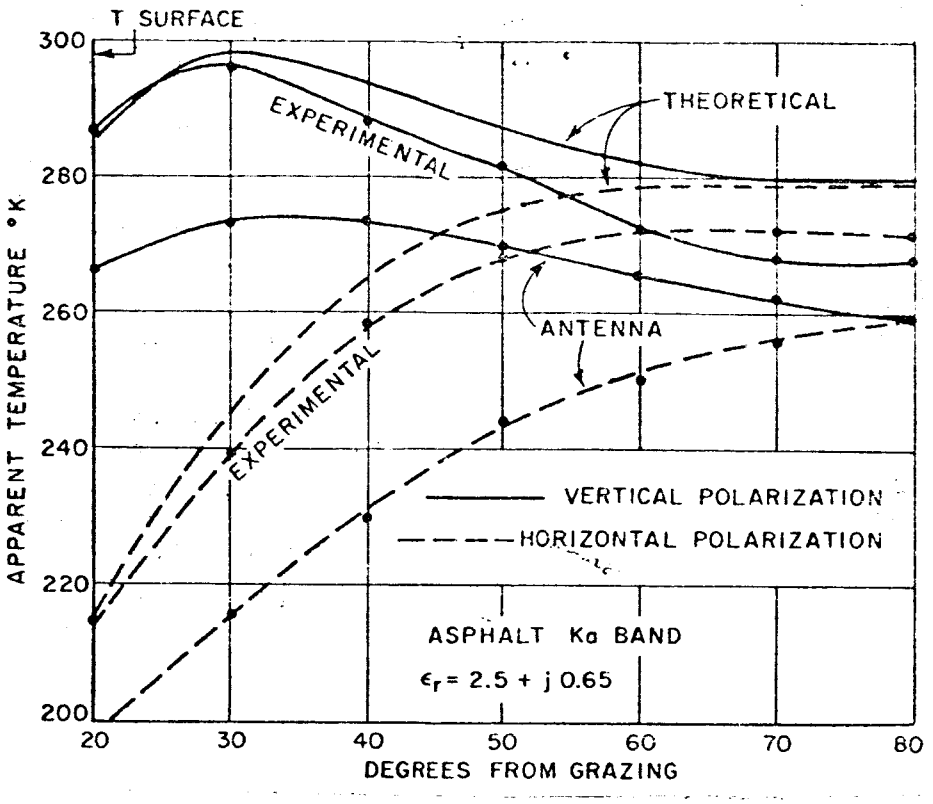

Fig. 17. Asphalt, Ka band.

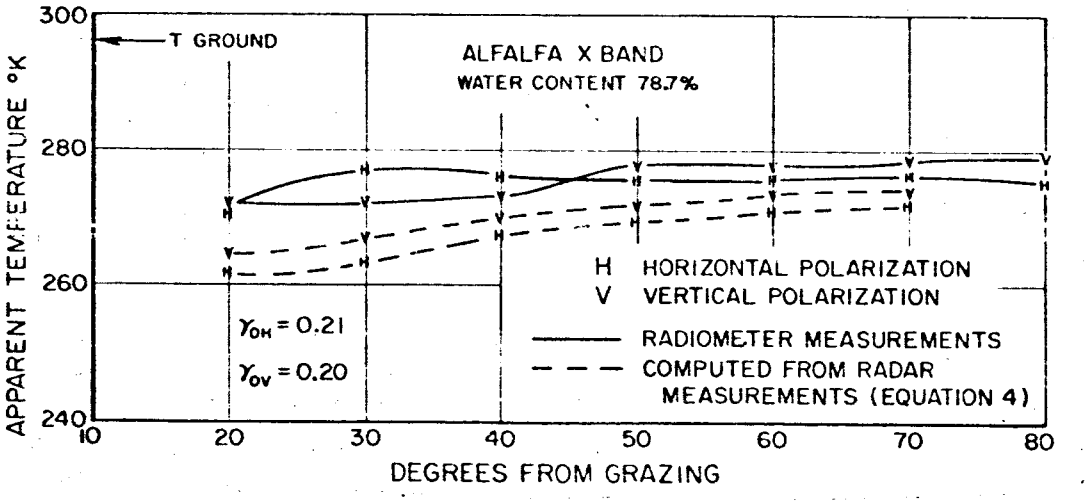

Fig. 18. Alfalfa, X band.

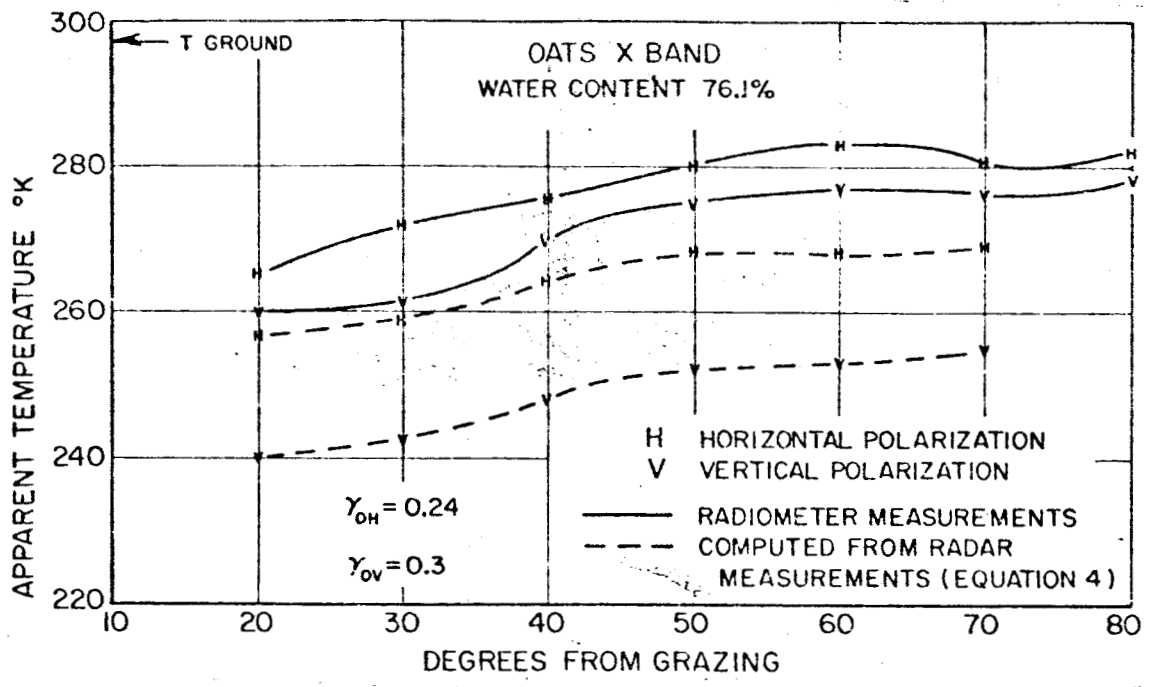

Fig. 19. Oats, X band.

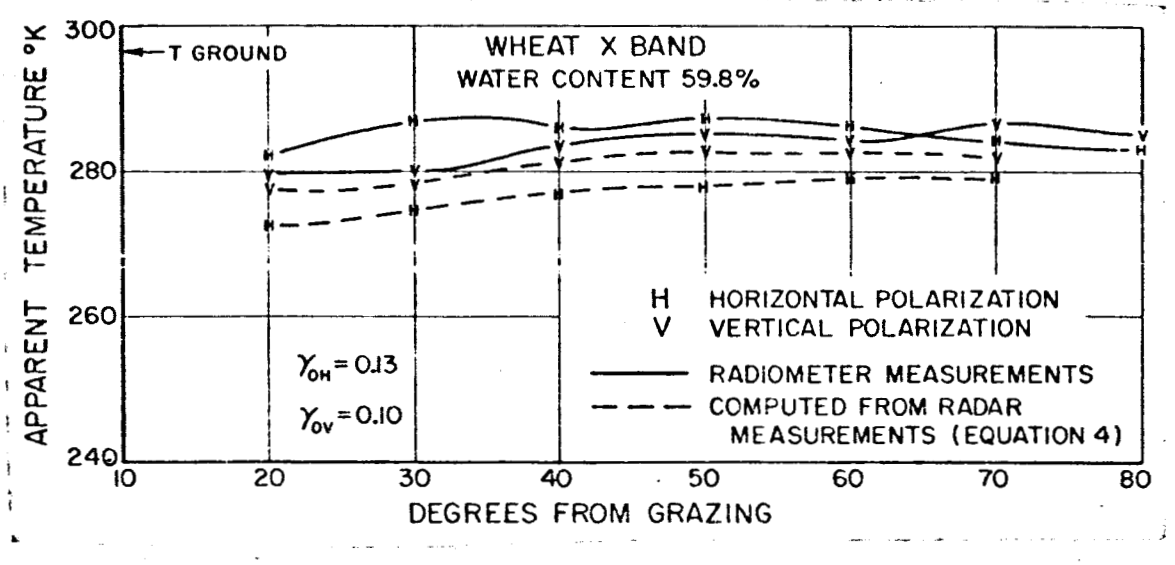

Fig. 20. Wheat, X band.

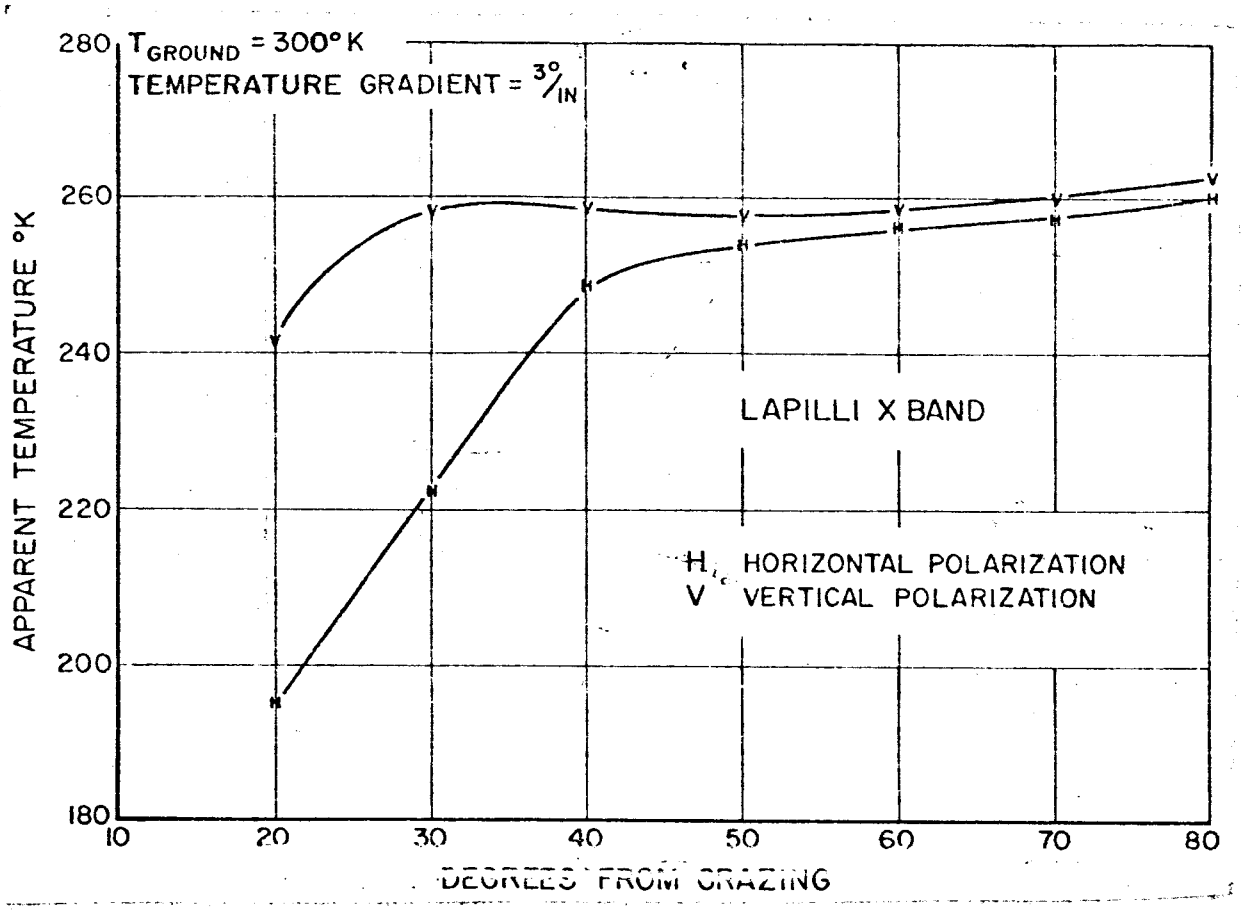

Fig. 21. Lapilli X band.

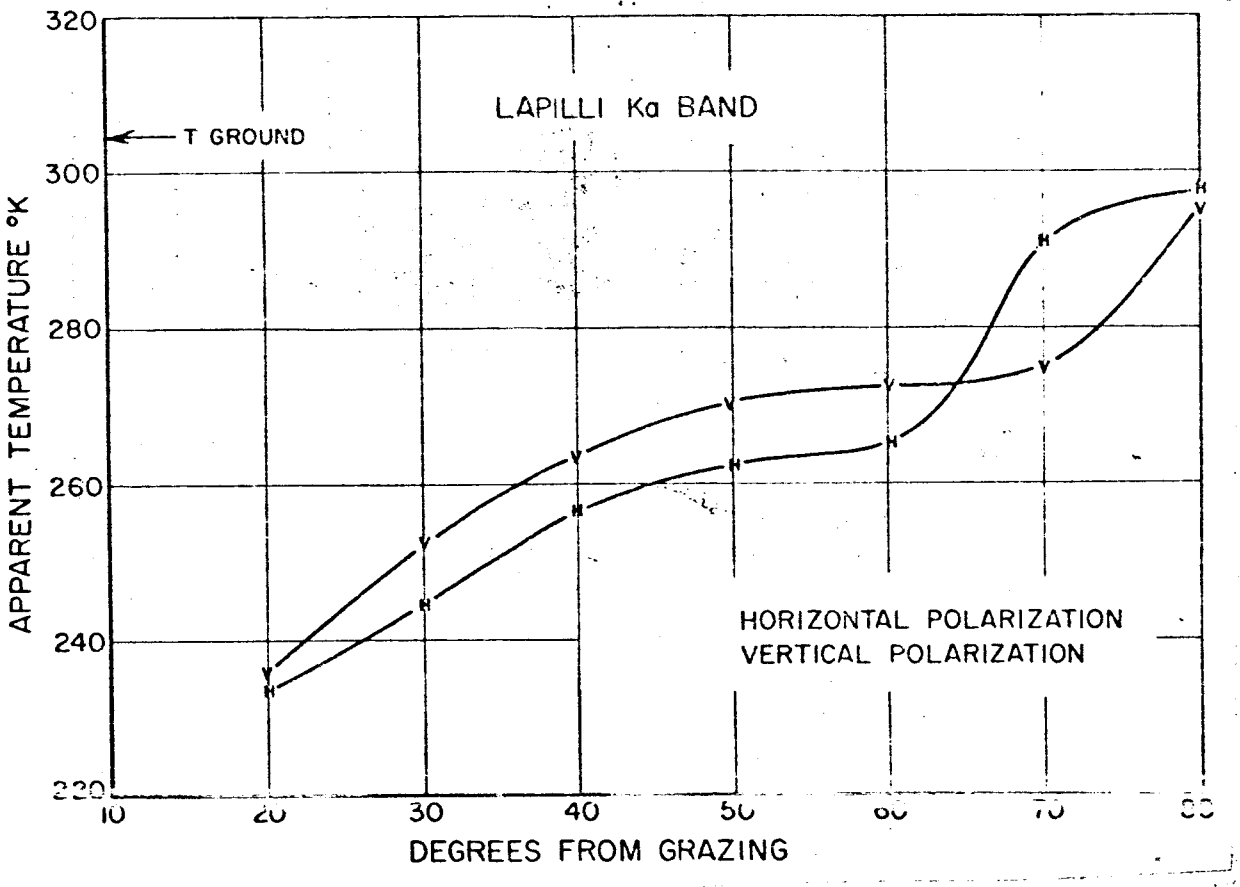

Fig. 22. Lapilli Ka band.

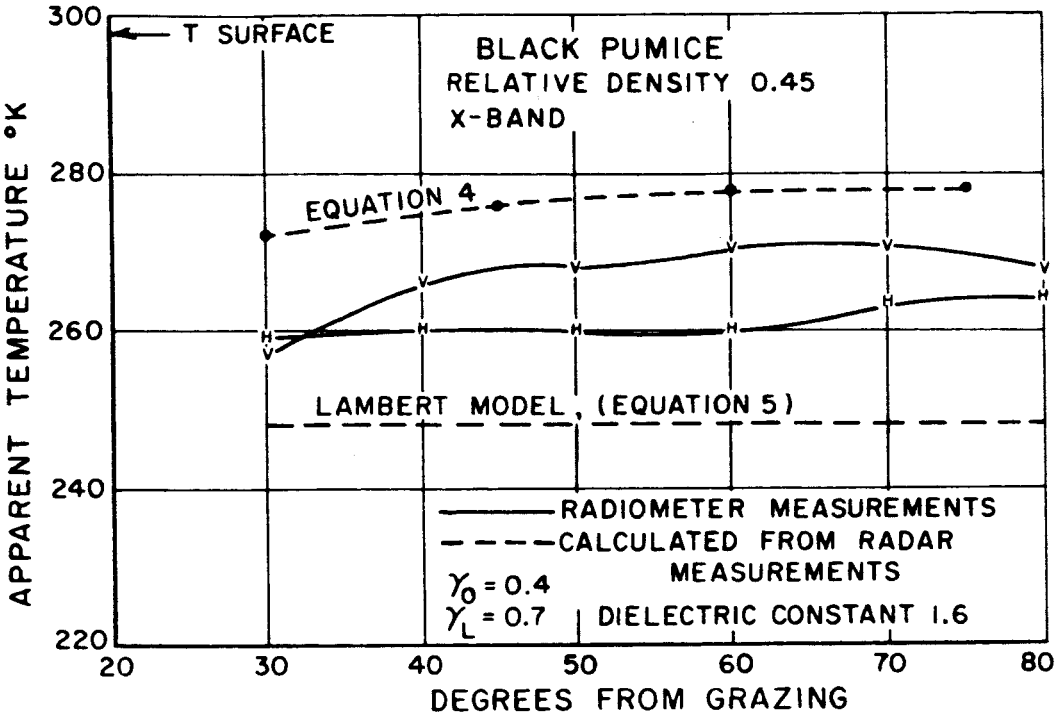

Fig. 23. Black pumice, X band.

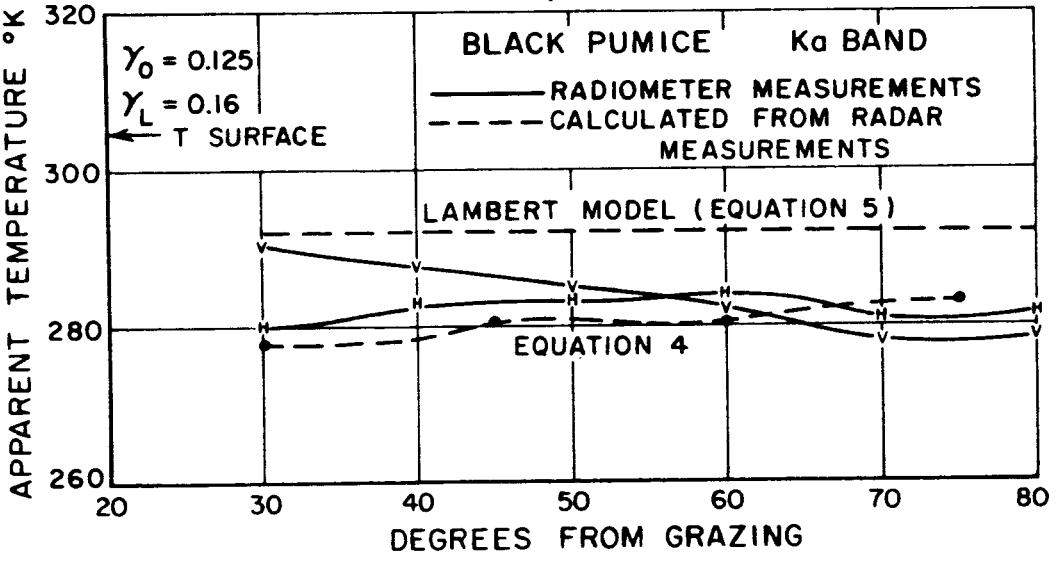

Fig. 24. Black pumice, Ka band.

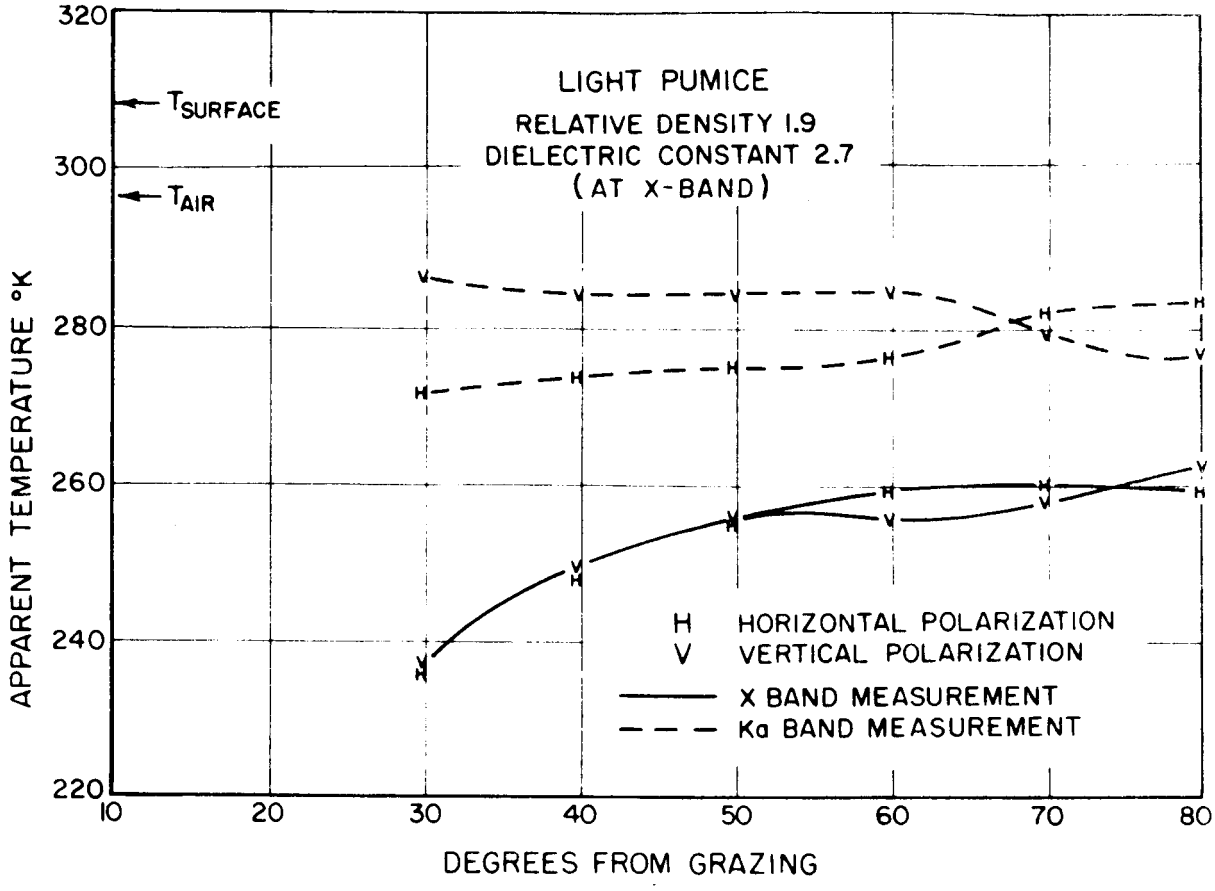

Fig. 25. Light pumice.

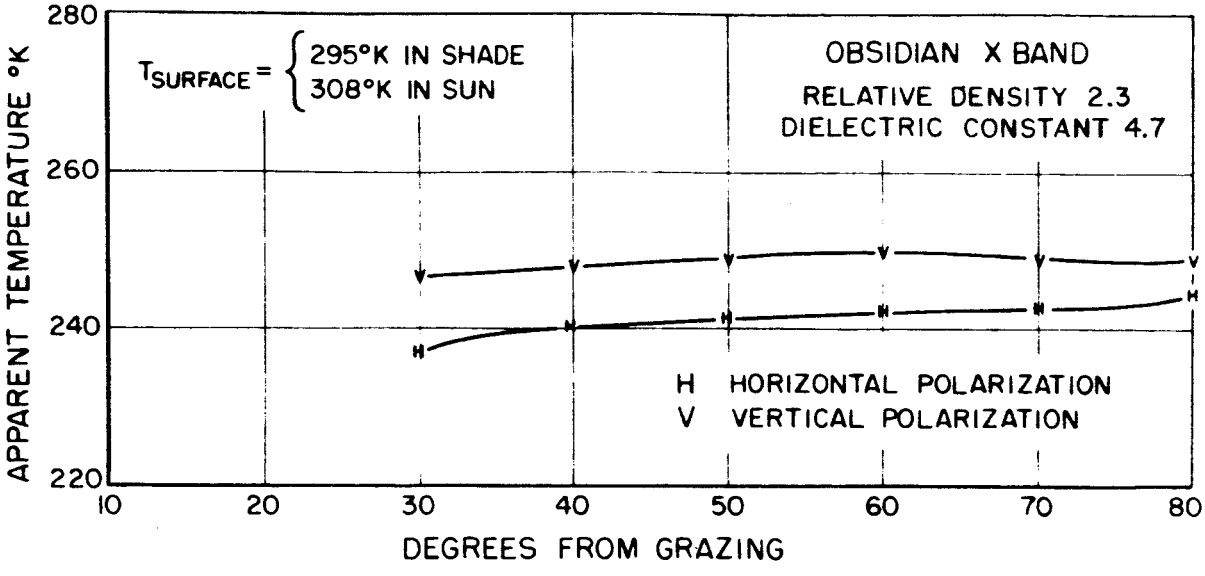

Fig. 26. Obsidian, X band.

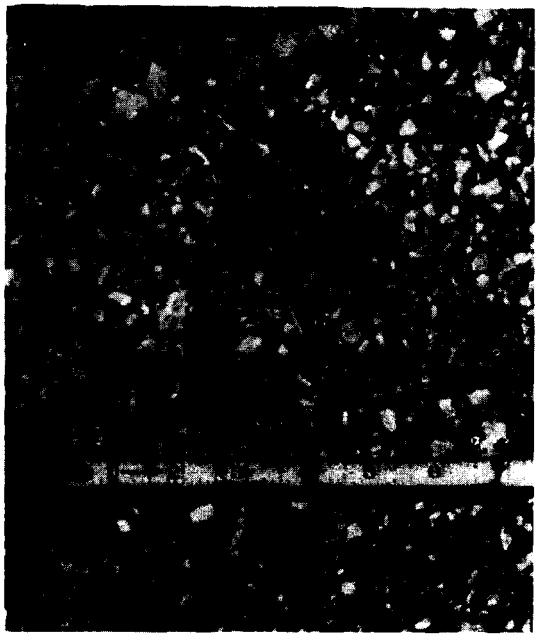

LAPILLI

DARK PUMICE

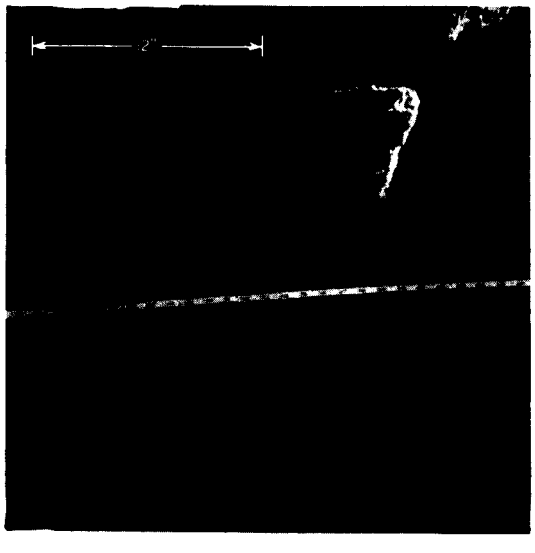

LIGHT PUMICE

OBSIDIAN

Fig. 27. Photographs of volcanic materials at Mono Craters, California.

APPENDIX II
DISCUSSION OF GEOMETRY PROBLEM

In order to evaluate the integral in Eq. (1) it is necessary to derive the geometrical relations between antenna co-ordinates and terrain geometry. Figure 5 shows the geometry of the problem to be solved.

Some object or terrain defines a ground based coordinate system XYZ, and the radiometric temperatures $T(\theta)$ are to be found in this system. The antenna views the terrain from some angle of incidence θ_o; the antenna then defines another coordinate system X' Y' Z' and the antenna pattern characteristics are known in this primed system. Without loss of generality the two systems can be oriented so that one coordinate is common to both systems (arbitrarily choose X' = X). Redrawing the two Cartesian systems as shown in Fig. 6 it is possible to express the unit vector $\hat{n}$ in both the primed and unprimed system and equate the two expressions.

$$\hat{n} = \hat{x} \sin\theta \cos\phi + \hat{y} \sin\theta \sin\phi + \hat{z} \cos\theta$$

$$\hat{n} = \hat{x}' \sin\theta' \cos\phi' + \hat{y}' \sin\theta' \sin\phi' + \hat{z}' \cos\theta'$$

where $\hat{x}, \hat{y}, \hat{z}$ and $\hat{x}', \hat{y}', \hat{z}'$ are unit vectors in the two systems.

The relationship between the primed and unprimed coordinates can then be expressed as

$$\hat{x}' = \hat{x}$$

$$\hat{y}' = \hat{y} \cos \theta_o - \hat{z} \sin \theta_o$$

$$\hat{z}' = \hat{y} \sin \theta_o + \hat{z} \cos \theta_o .$$

Equating $\hat{n}$ in both systems and substituting for the coordinate vector yields

$$\sin \theta \cos \phi = \sin \theta' \cos \phi'$$

$$\sin \theta \cos \phi = \cos \theta_o \sin \theta' \sin \phi' + \sin \theta_o \cos \theta'$$

$$\cos \theta = \cos \theta_o \cos \theta' - \sin \theta_o \sin \theta \sin \phi' .$$

After some algebraic manipulation, the desired relationships between the antenna system and the terrain system are

$$\phi = \tan^{-1} \left[\frac{\cos \theta_o \sin \theta' \sin \phi' + \sin \theta_o \cos \theta'}{\sin \theta' \cos \phi'} \right]$$

$$\theta = \tan^{-1} \left[\frac{\sin \theta' \cos \phi'}{\cos \phi (\cos \theta_o \cos \theta' - \sin \theta_o \sin \theta' \sin \phi')} \right] .$$

APPENDIX III
COMPUTER PROGRAM

The computer solution to obtain radiometric temperatures from the measured antenna temperatures was done in two parts. From the equation

$$T_{ant} = \frac{\int_0^{2\pi}\int_0^{\pi} T(\theta) f(\theta'\phi')\, d\Omega'}{\int_0^{2\pi}\int_0^{\pi} f(\theta'\phi')\, d\Omega'}$$

it is obvious that the normalizing integral in the denominator is determined by the antenna characteristics and it need be found only once for a given antenna. However the numerator contains $T(\theta)$, the radiometric temperature distribution, which changes for each terrain; it is more efficient to divide the problem into two programs so that the normalizing factor is only computed once.

```
***     RUN
***     SCATRAN
C           SOLUTION OF INTEGRAL EQUATION TO FIND RAY TEMP.-
            DIMENSION(THETP(150),FPNU(150),TEMP(25),TALSO(25),TANT(25))-
  SA        READINPUT,X,(DENOM)-
F X         (E16.8)-
            READINPUT,FMA,(NN)-
F FMA       (I10)-
            DOTHROUGH(S20),N=1,1,N.LE.NN-
            READ INPUT,Y,(THETP(N))-
F Y         (25(G.0))-
  S20       FPNU(N)=EXP.(-2.3*FDEP/10.)-
            CF=3.141592/180.-
            READINPUT,FMA,(JJ)-
            DOTHROUGH(S15),NSETS=1,1,NSETS.LE.JJ-
            DOTHROUGH(S10),I=1,1,I.LE.19-
            READ INPUT,Y,(ANGLE,TEMP(I))-
  S10       TALSO(I)=TEMP(I)-
            DOTHROUGH(S25),ITER=1,1,ITER.LE.2-
            DO THROUGH(S35),THETO=0.,10.,THETO.LE.180.-
            THORA=THETO*CF-
            SUMAR=0.-
            U=SIN.(THORA)-
            V=COS.(THORA)-
            DOTHROUGH(S40),N=2,1,N.LE.NN-
            AREA=0.-
            THPRA=THETP(N)*CF
            COSTP=COS.(THPRA)*V-
            Z=SIN.(THPRA)-
            SING=U*Z-
            AREAP=FPNU(N)*Z*10.*CF*(THETP(N)-THETP(N-1))*CF-
            DO THROUGH (S45),PHI=0.,10.,PHI.LE.360.-
            COSTH=COSTP-SIN.(PHI*CF)*SING-
            TANTH=(SQRT.(1.-COSTH*COSTH))/COSTH-
            THDEG=FATAN2.(1.,1./TANTH)/CF-
            ITHET=THDEG-
            ITHLO=(ITHET/10)*10-
            I=(ITHLO/10)+1-
            THLO=ITHLO-
            TAVE=TEMP(I)+((THDEG-THLO)/10.)*(TEMP(I+1)-TEMP(I))-
  S45       AREA=AREA+TAVE*AREAP-
  S40       SUMAR=SUMAR+AREA-
            ITHETO=THETO-
            I=ITHETO/10+1-
  S35       TANT(I)=SUMAR/DENOM-
            DO THROUGH(S5),I=1,1,I.LE.19-
            TEMP(I)=2.*TEMP(I)-TANT(I)-
  S5        WRITE OUTPUT,1,(TEMP(I))-
  S25       CONTINUE-
            DO THROUGH(S99),I=12,1,I.LE.19-
            TRAY=(TEMP(I)-TANT(I))/2.+TALSO(I)-
            THETA=10*(I-1)-
  S99       WRITE OUTPUT,1,(THETA,TALSO(I),TANT(I),TRAY)-
  S15       CONTINUE-
            CALLSUBROUTINE()=ENDJOB.()-
            ENDPROGRAM(SA)-
***     DATA
```

```
 ***      RUN
 ***      SCATRAN
C             NORMALIZING INTEGRAL-
              DIMENSION(THETP(150),FDBP(150),TEMP(25))-
 SA           READINPUT,FMA,(NN)-
F FMA         (I8)-
              CF=3.1415927/180.-
              DOTHROUGH(S20),N=1,1,N.LE.NN-
  S20         READINPUT,Y,(THETP(N),FDBP(N))-
F Y           (2F16.1)-
              SUMAR=0.-
              DOTHROUGH(S40),N=2,1,N.LE.NN-
              AREA=0.-
              THPRA=THETP(N)*CF          -
              FPNU=EXPE.((-2.3*FDBP(N)/10.))-
              AREA=FPNU*SIN.(THPRA)*10.*CF*(THETP(N)-THETP(N-1))*CF-
  S40         SUMAR=SUMAR+AREA*36.-
              WRITEOUTPUT,1,(SUMAR)-
              CALLSUBROUTINE()=ENDJOB.()-
              ENDPROGRAM(SA)-
 ***      DATA
```

APPENDIX IV
ANTENNA PATTERNS

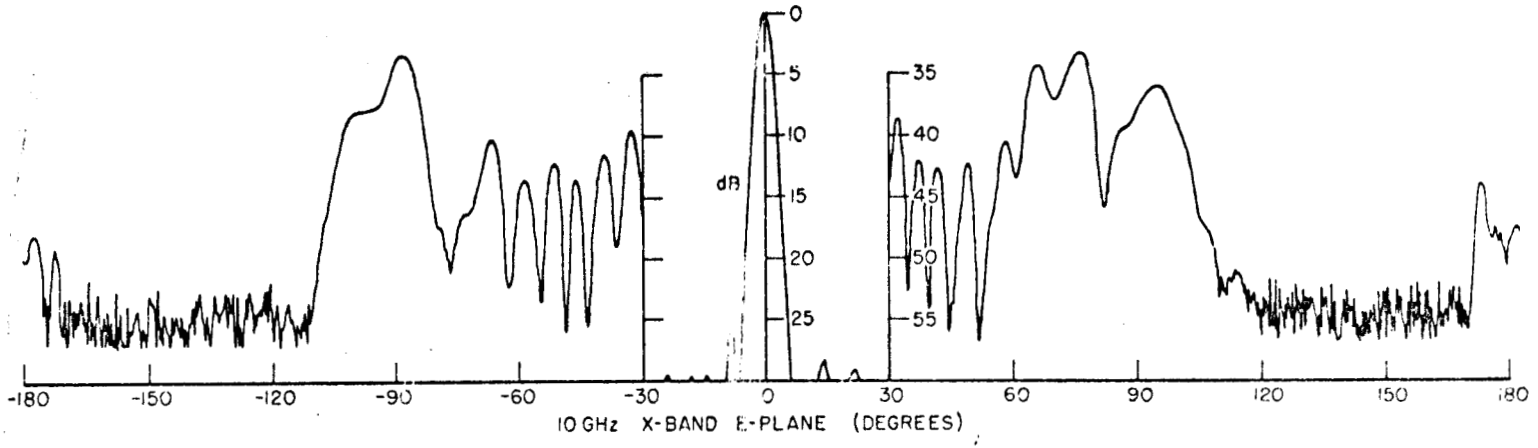

Fig. 28. Antenna pattern.

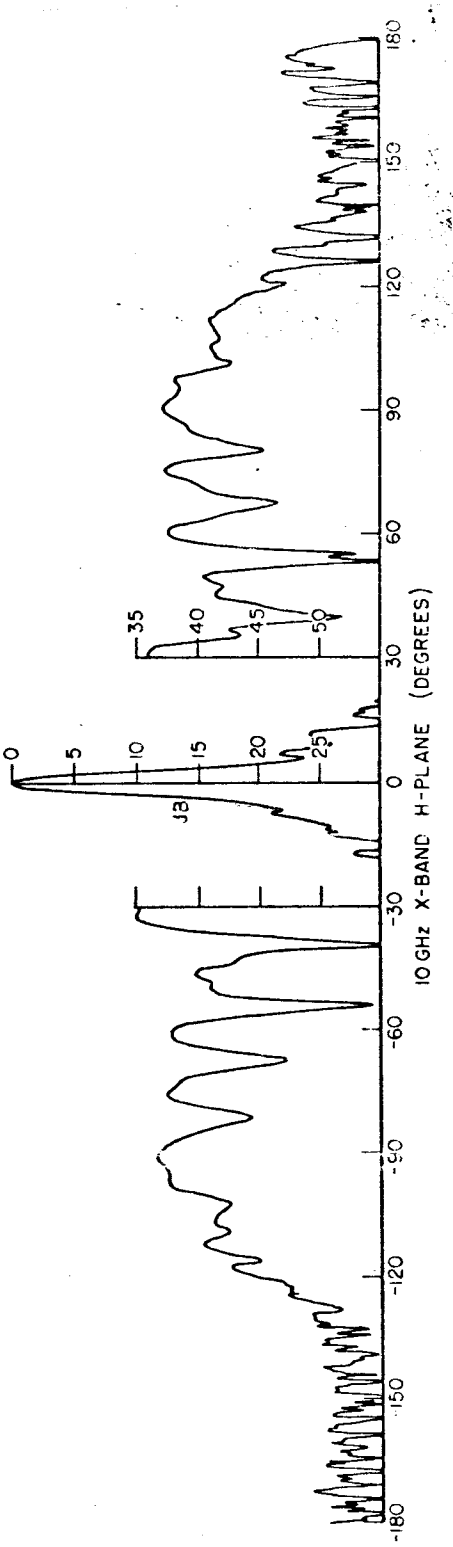

Fig. 24. Antenna pattern.

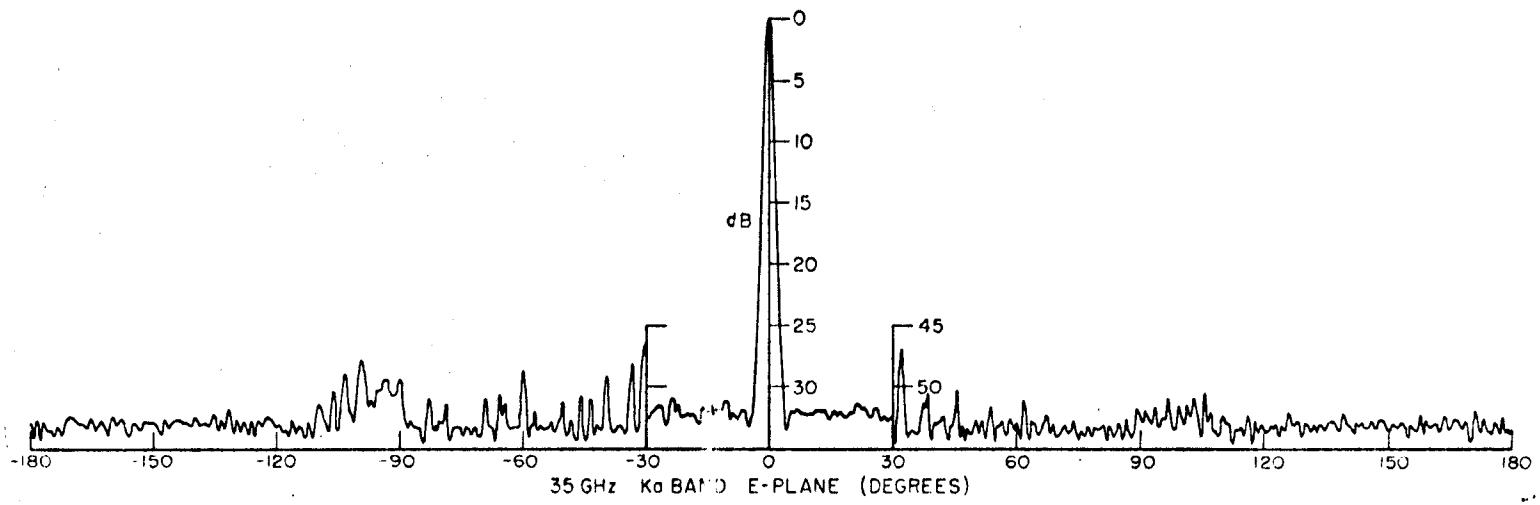

Fig. 30. Antenna pattern.

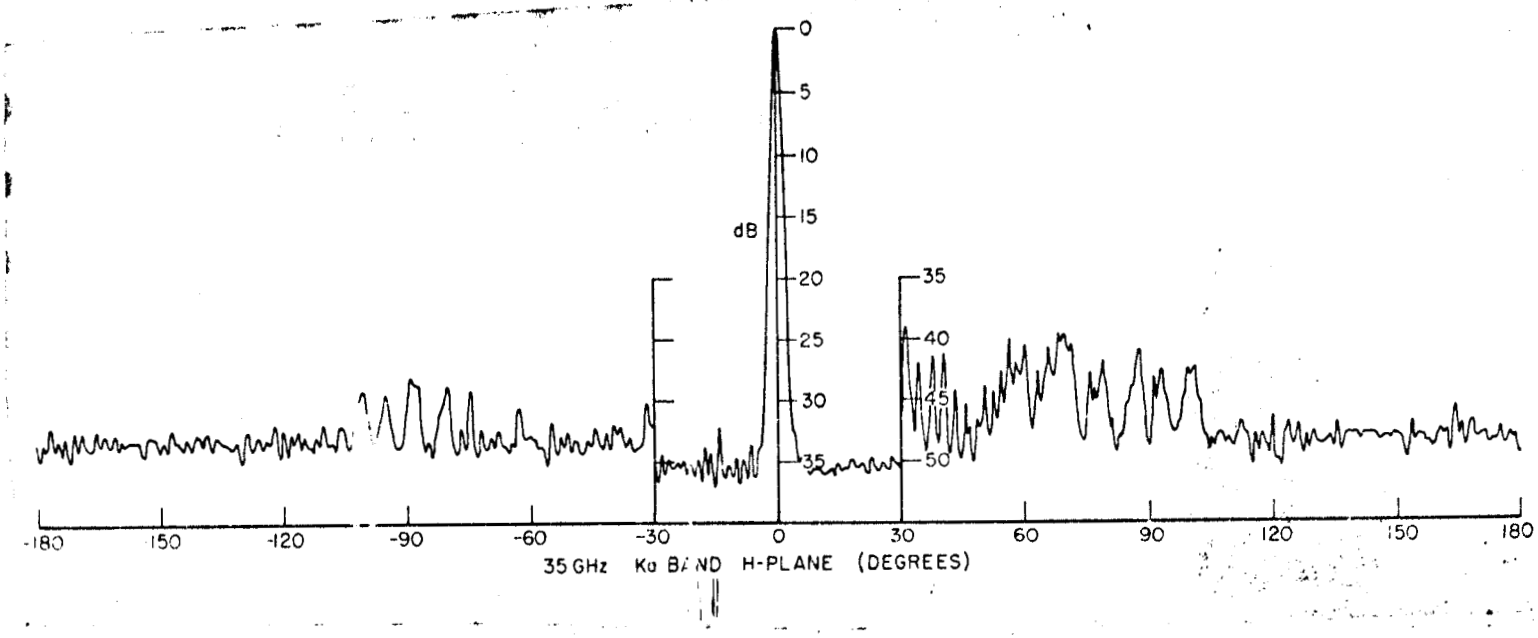

Fig. 31. Antenna pattern.